NLO inclusive J/ψ photoproduction at large P_T at HERA and the EIC

Carlo Flore

Laboratoire de Physique des 2 Infinis
Irène Joliot-Curie (IJCLab), CNRS, Orsay

DIS 2021
(virtual meeting)
13 Apr 2021

CF, J.-P. Lansberg, H.-S. Shao, Y. Yedelkina, Phys. Lett. B 811 (2020) 135926

Quarkonium Production Model

Phys.Rept. 889 (2020) 1-106 & EPJC (2016) 76:107 for reviews

Quarkonium Production Model

Phys.Rept. 889 (2020) 1-106 & EPJC (2016) 76:107 for reviews

- No agreement on which mechanism is dominant

[see C. Van Hulse talk on Monday]

Quarkonium Production Model

Phys.Rept. 889 (2020) 1-106 & EPJC (2016) 76:107 for reviews

- No agreement on which mechanism is dominant

  [see C. Van Hulse talk on Monday]

- Differences in the treatment of the hadronization

Quarkonium Production Model

Phys.Rept. 889 (2020) 1-106 & EPJC (2016) 76:107 for reviews

- No agreement on which mechanism is dominant

  [see C. Van Hulse talk on Monday]

- Differences in the treatment of the hadronization
- 3 common models:

Quarkonium Production Model

Phys.Rept. 889 (2020) 1-106 & EPJC (2016) 76:107 for reviews

- No agreement on which mechanism is dominant

  [see C. Van Hulse talk on Monday]

- Differences in the treatment of the hadronization
- 3 common models:
  1. Color Singlet Model:

     hadronization w/o gluon emission; colour and spin are preserved during the hadronization

Quarkonium Production Model

Phys.Rept. 889 (2020) 1-106 & EPJC (2016) 76:107 for reviews

- No agreement on which mechanism is dominant

  [see C. Van Hulse talk on Monday]

- Differences in the treatment of the hadronization
- 3 common models:
  1. Color Singlet Model:

     hadronization w/o gluon emission; colour and spin are preserved during the hadronization
  2. NRQCD and Color Octet Mechanism:

     higher Fock states of the mesons taken into account; $Q\bar{Q}$ can be produced in octet states with different quantum number as the meson;

Quarkonium Production Model

Phys.Rept. 889 (2020) 1-106 & EPJC (2016) 76:107 for reviews

- No agreement on which mechanism is dominant

  [see C. Van Hulse talk on Monday]

- Differences in the treatment of the hadronization
- 3 common models:
  1. Color Singlet Model:
     hadronization w/o gluon emission; colour and spin are preserved during the hadronization
  2. NRQCD and Color Octet Mechanism:
     higher Fock states of the mesons taken into account; $Q\bar{Q}$ can be produced in octet states with different quantum number as the meson;
  3. Color Evaporation Model:
     based on quark-hadron duality;
     only the invariant mass matters; semi-soft gluons emissions;
     color-wise decorrelated $c\bar{c}$ prod. and hadr.

Leading P_T approximation of NLO $J/\psi + g$: NLO*

P. Artoisenet *et al.*, **PRL 101 (2008) 152001, J.-P. Lansberg, EPJC 61 (2009) 693 & PLB 679 (2009) 340**

Leading P_T approximation of NLO $J/\psi + g$: NLO*

P. Artoisenet *et al.*, PRL 101 (2008) 152001, J.-P. Lansberg, EPJC 61 (2009) 693 & PLB 679 (2009) 340

- NLO* only contains the real-emission contributions with an IR cut-off, $\sqrt{s_{ij}^{\min}}$, and is expected to account for the leading P_T contributions at NLO (P_T^{-6})

Leading P_T approximation of NLO $J/\psi + g$: NLO*

P. Artoisenet *et al.*, PRL 101 (2008) 152001, J.-P. Lansberg, EPJC 61 (2009) 693 & PLB 679 (2009) 340

- NLO* only contains the real-emission contributions with an IR cut-off, $\sqrt{s_{ij}^{\min}}$, and is expected to account for the leading P_T contributions at NLO (P_T^{-6})
- It has been succesfully checked against full NLO computations for $P_T > 3$ GeV

Leading P_T approximation of NLO $J/\psi + g$: NLO*

P. Artoisenet *et al.*, PRL 101 (2008) 152001, J.-P. Lansberg, EPJC 61 (2009) 693 & PLB 679 (2009) 340

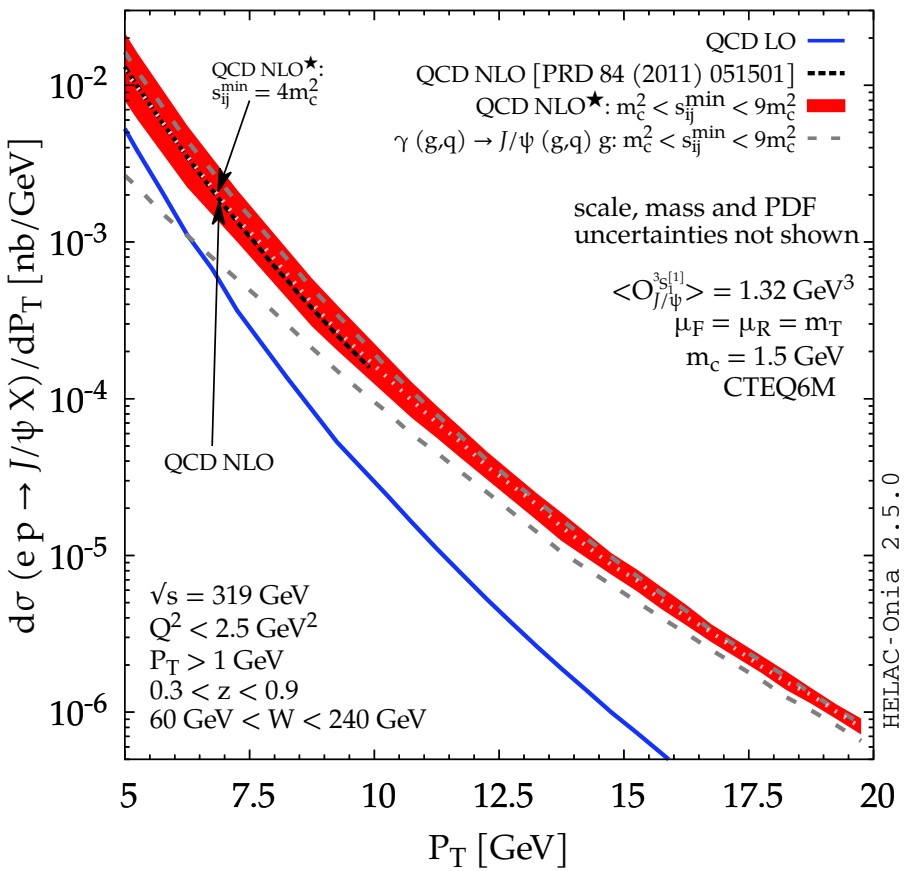

CSM QCD NLO from **PRD 84 (2011) 051501**

- NLO* only contains the real-emission contributions with an IR cut-off, $\sqrt{s_{ij}^{min}}$, and is expected to account for the leading P_T contributions at NLO (P_T^{-6})
- It has been succesfully checked against full NLO computations for $P_T > 3$ GeV

Leading P_T approximation of NLO $J/\psi + g$: NLO*

P. Artoisenet *et al.*, PRL 101 (2008) 152001, J.-P. Lansberg, EPJC 61 (2009) 693 & PLB 679 (2009) 340

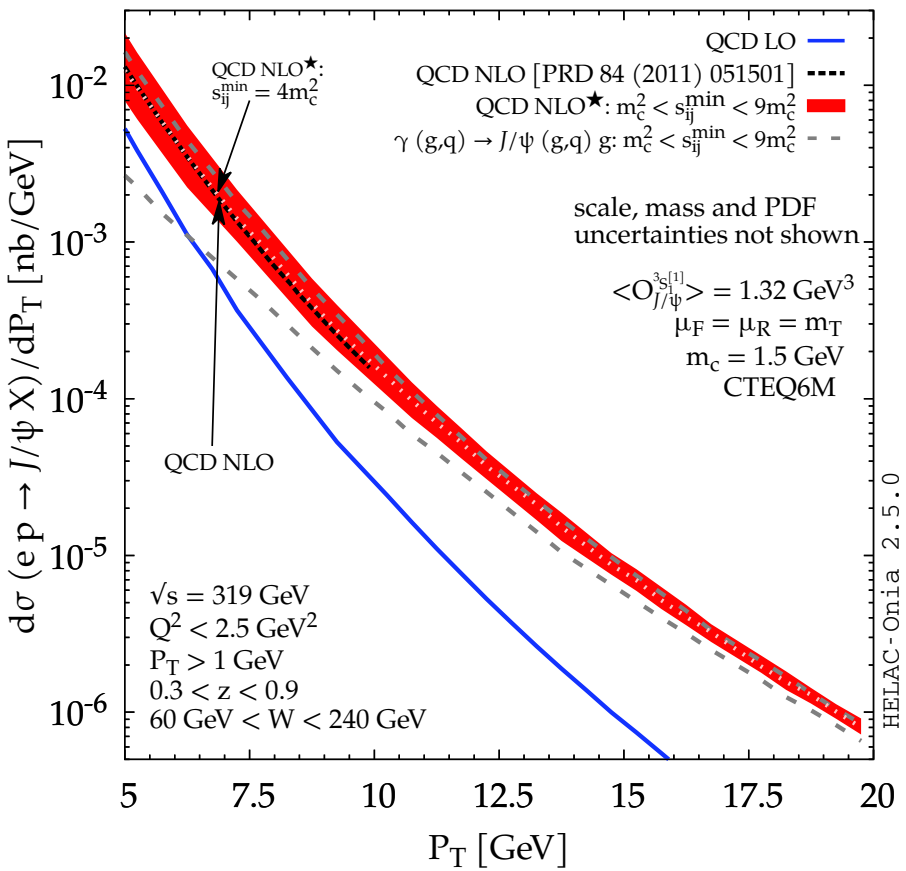

CSM QCD NLO from **PRD 84 (2011) 051501**

- NLO* only contains the real-emission contributions with an IR cut-off, $\sqrt{s_{ij}^{min}}$, and is expected to account for the leading P_T contributions at NLO (P_T^{-6})
- It has been succesfully checked against full NLO computations for $P_T > 3$ GeV
- $\sqrt{s_{ij}^{min}}/m_c \in [1{:}3]$ suitable for our study; $\sqrt{s_{ij}^{min}} = 2m_c$ remarkably reproduces NLO results

Leading P_T approximation of NLO $J/\psi + g$: NLO*

P. Artoisenet *et al.*, PRL 101 (2008) 152001, J.-P. Lansberg, EPJC 61 (2009) 693 & PLB 679 (2009) 340

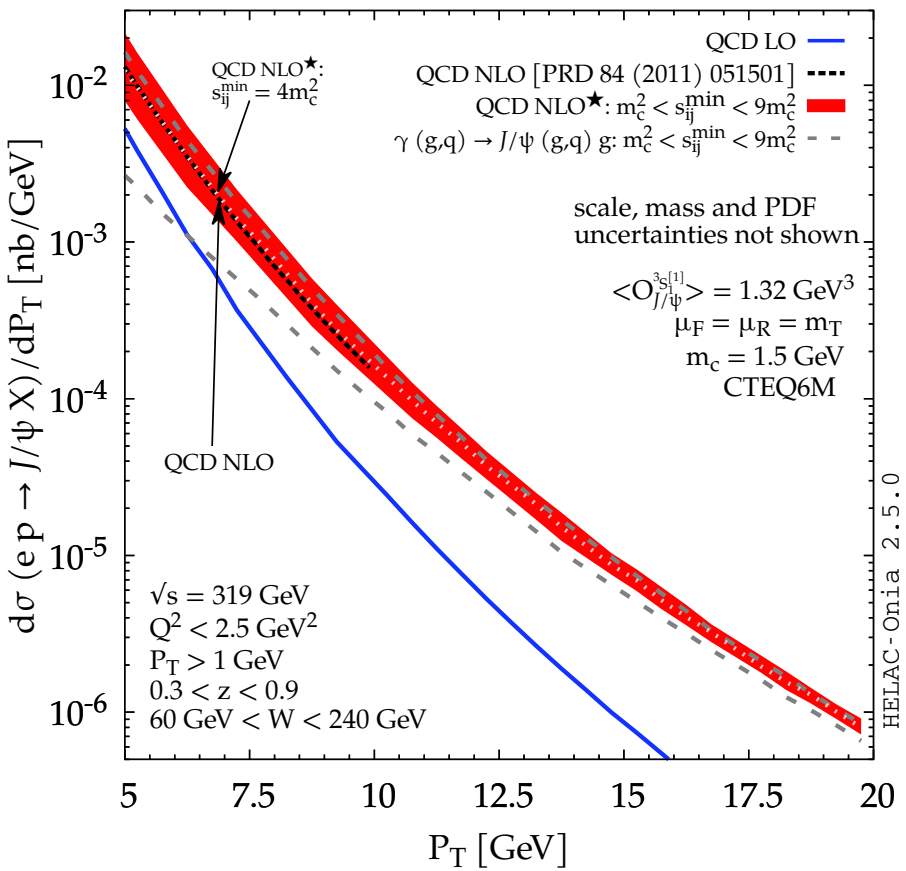

CSM QCD NLO from **PRD 84 (2011) 051501**

- NLO* only contains the real-emission contributions with an IR cut-off, $\sqrt{s_{ij}^{min}}$, and is expected to account for the leading P_T contributions at NLO (P_T^{-6})
- It has been succesfully checked against full NLO computations for $P_T > 3$ GeV
- $\sqrt{s_{ij}^{min}}/m_c \in [1{:}3]$ suitable for our study; $\sqrt{s_{ij}^{min}} = 2m_c$ remarkably reproduces NLO results

Let's revisit HERA data!

Revisiting HERA data (I)

CF, J.-P. Lansberg, H.-S. Shao, Y. Yedelkina, PLB 811 (2020) 135926

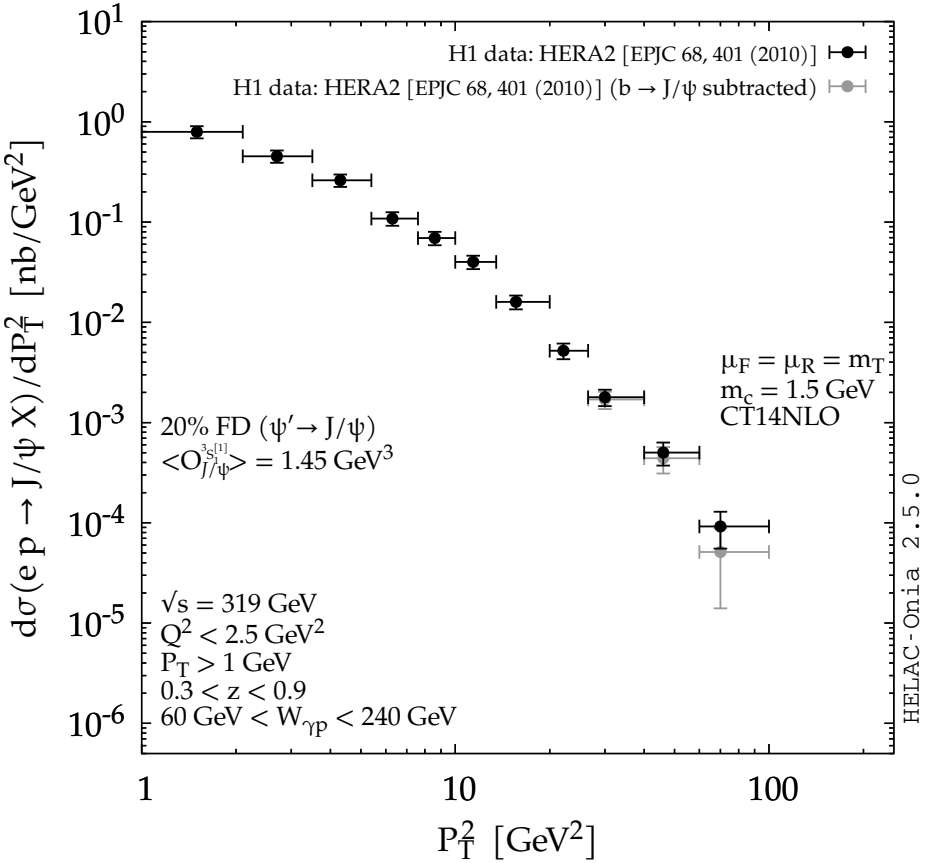

All the computations are done with HELAC-ONIA **[H.-S. Shao, CPC198 (2016) 238]**. See also `https://nloaccess.in2p3.fr`

Revisiting HERA data (I)

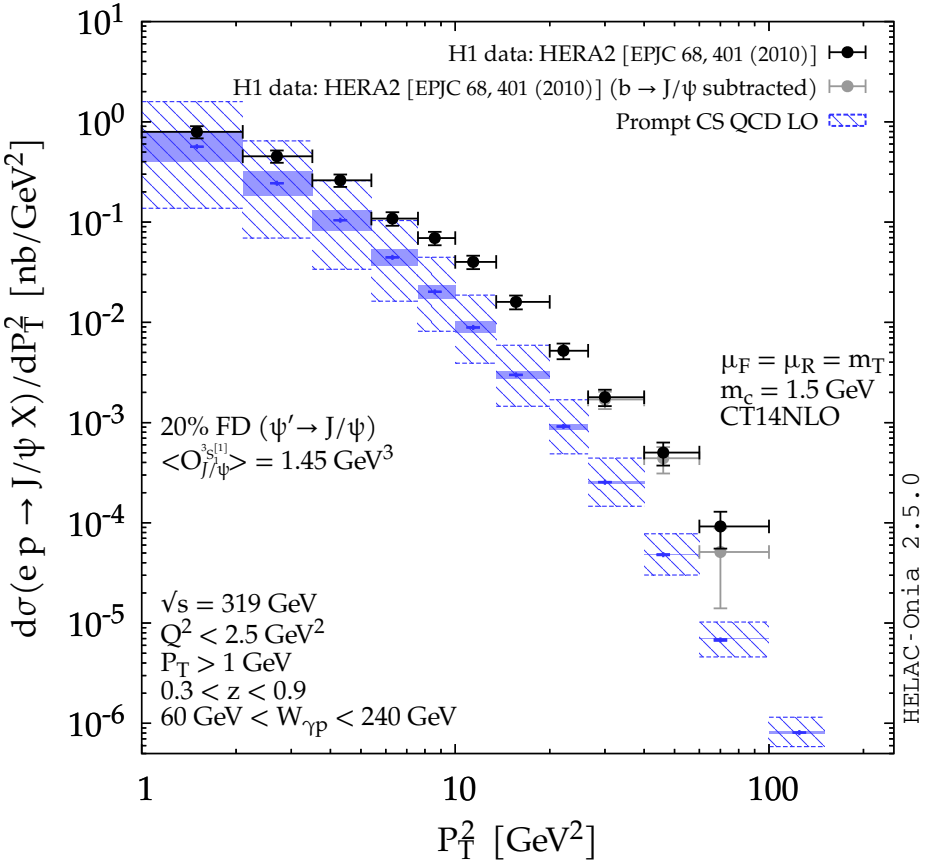

CF, J.-P. Lansberg, H.-S. Shao, Y. Yedelkina, PLB 811 (2020) 135926

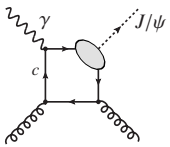

$$\gamma + g \to \psi + g \,@\, \alpha\alpha_s^2$$

All the computations are done with HELAC-Onia **[H.-S. Shao, CPC198 (2016) 238]**. See also `https://nloaccess.in2p3.fr`
Scale and mass uncertainties are shown by the hatched and solid bands respectively.

[The quark and antiquark attached to the ellipsis are taken as on-shell and their relative velocity v is set to zero.]

Revisiting HERA data (I)

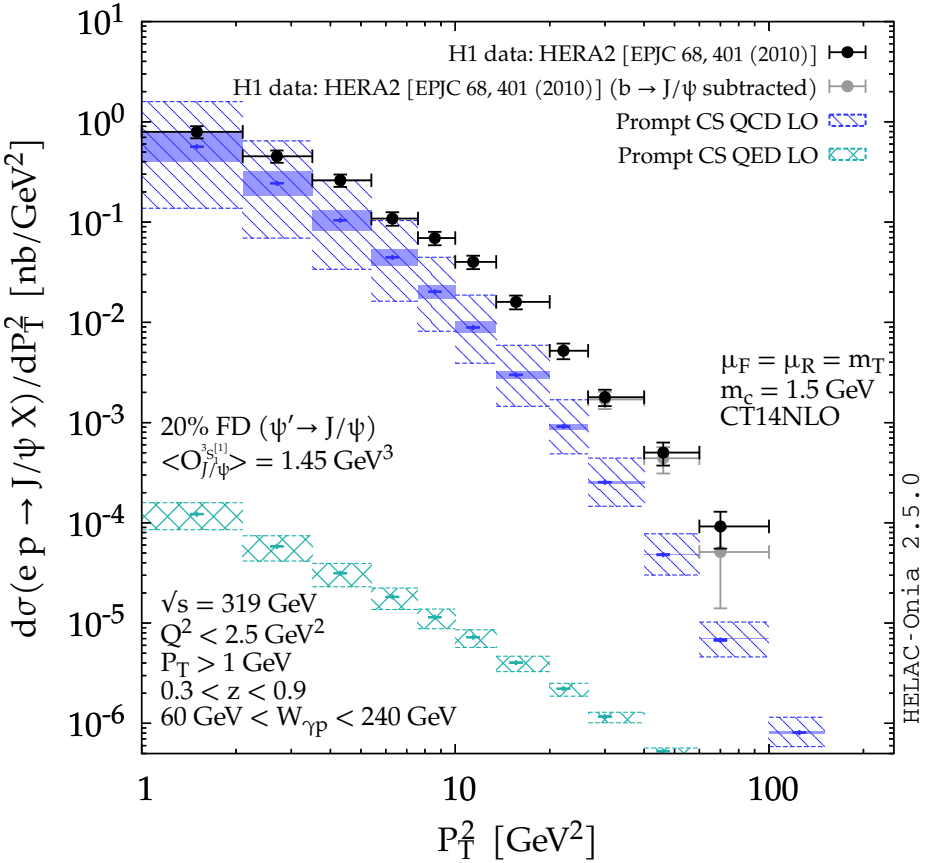

CF, J.-P. Lansberg, H.-S. Shao, Y. Yedelkina, PLB 811 (2020) 135926

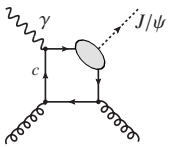

$\gamma + g \to \psi + g \,@\, \alpha\alpha_s^2$

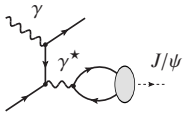

$\gamma + q \to \psi + q \,@\, \alpha^3$ [NEW!]

All the computations are done with HELAC-Onia **[H.-S. Shao, CPC198 (2016) 238]**. See also `https://nloaccess.in2p3.fr`
Scale and mass uncertainties are shown by the hatched and solid bands respectively.

[The quark and antiquark attached to the ellipsis are taken as on-shell and their relative velocity v is set to zero.]

Revisiting HERA data (I)

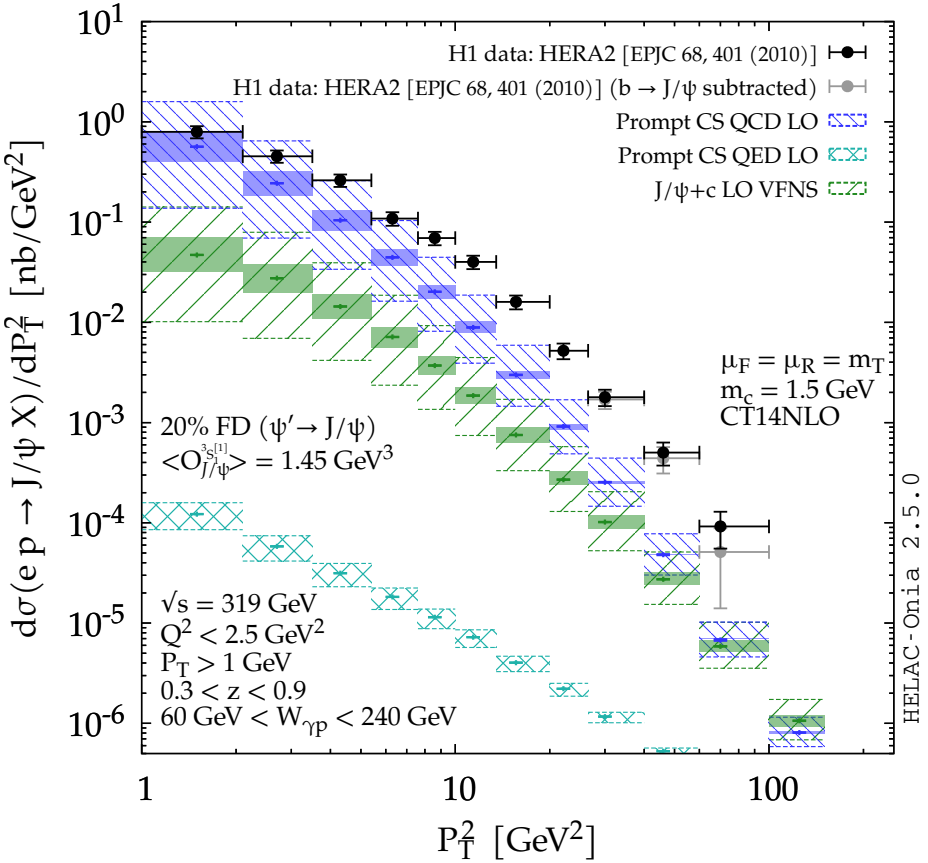

CF, J.-P. Lansberg, H.-S. Shao, Y. Yedelkina, PLB 811 (2020) 135926

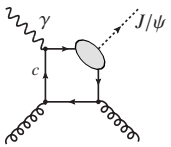

$\gamma + g \to \psi + g \,@\, \alpha\alpha_s^2$

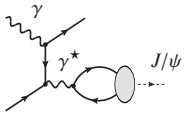

$\gamma + q \to \psi + q \,@\, \alpha^3$ [NEW!]

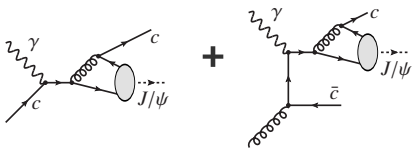

$$\begin{cases} \gamma + c \to \psi + c \,@\, \alpha\alpha_s^2 & \text{(4FS)} \\ \gamma + g \to \psi + c + \bar{c} \,@\, \alpha\alpha_s^3 & \text{(3FS)} \end{cases}$$ [also NEW!]

All the computations are done with HELAC-Onia [H.-S. Shao, CPC198 (2016) 238]. See also `https://nloaccess.in2p3.fr`
Scale and mass uncertainties are shown by the hatched and solid bands respectively.

[The quark and antiquark attached to the ellipsis are taken as on-shell and their relative velocity v is set to zero.]

Revisiting HERA data (I)

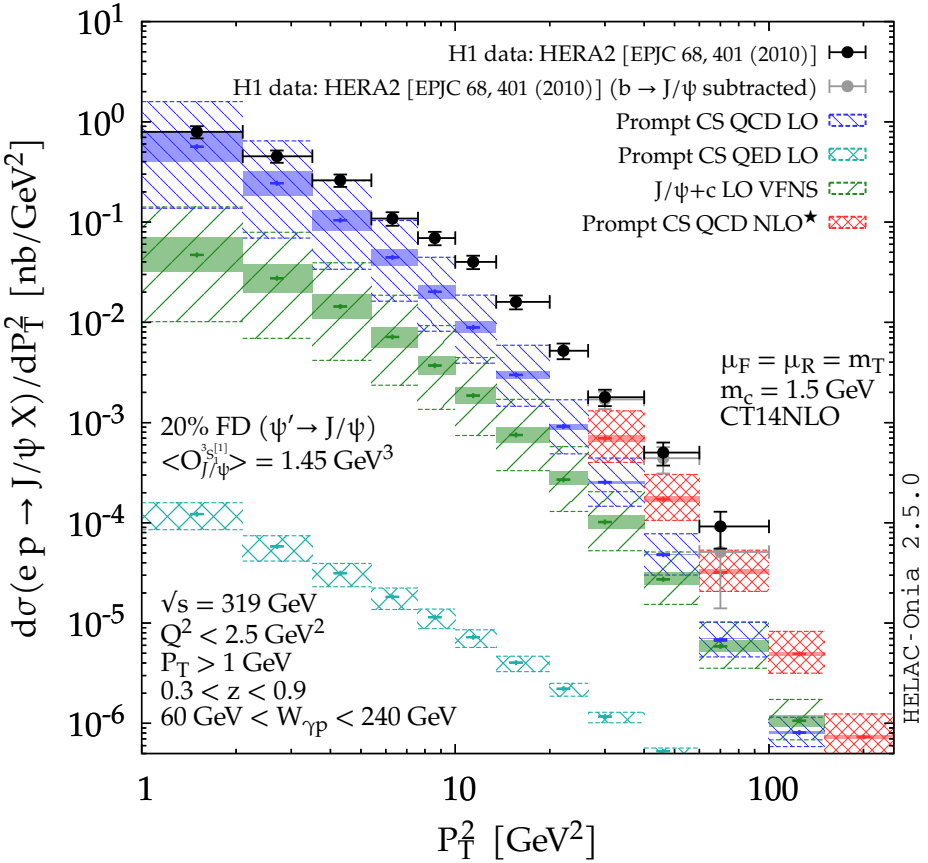

CF, J.-P. Lansberg, H.-S. Shao, Y. Yedelkina, PLB 811 (2020) 135926

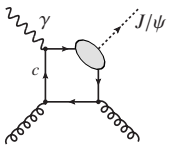

$\gamma + g \to \psi + g \,@\, \alpha\alpha_s^2$

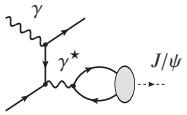

$\gamma + q \to \psi + q \,@\, \alpha^3$ [NEW!]

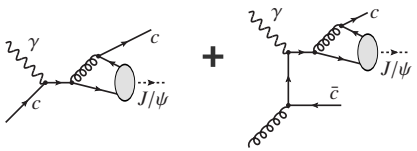

$$\begin{cases} \gamma+c\to\psi+c \,@\, \alpha\alpha_s^2 & \text{(4FS)} \\ \gamma+g\to\psi+c+\bar{c} \,@\, \alpha\alpha_s^3 & \text{(3FS)} \end{cases}$$ [also NEW!]

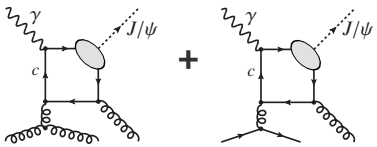

$$\begin{cases} \gamma+g\to\psi+g+g \,@\, \alpha\alpha_s^3 \\ \gamma+q\to\psi+g+q \,@\, \alpha\alpha_s^3 \end{cases}$$

[+ $\gamma + g \to \psi + g$]

All the computations are done with HELAC-ONIA [H.-S. Shao, CPC198 (2016) 238]. See also `https://nloaccess.in2p3.fr`
Scale and mass uncertainties are shown by the hatched and solid bands respectively.

[The quark and antiquark attached to the ellipsis are taken as on-shell and their relative velocity v is set to zero.]

Revisiting HERA data (I)

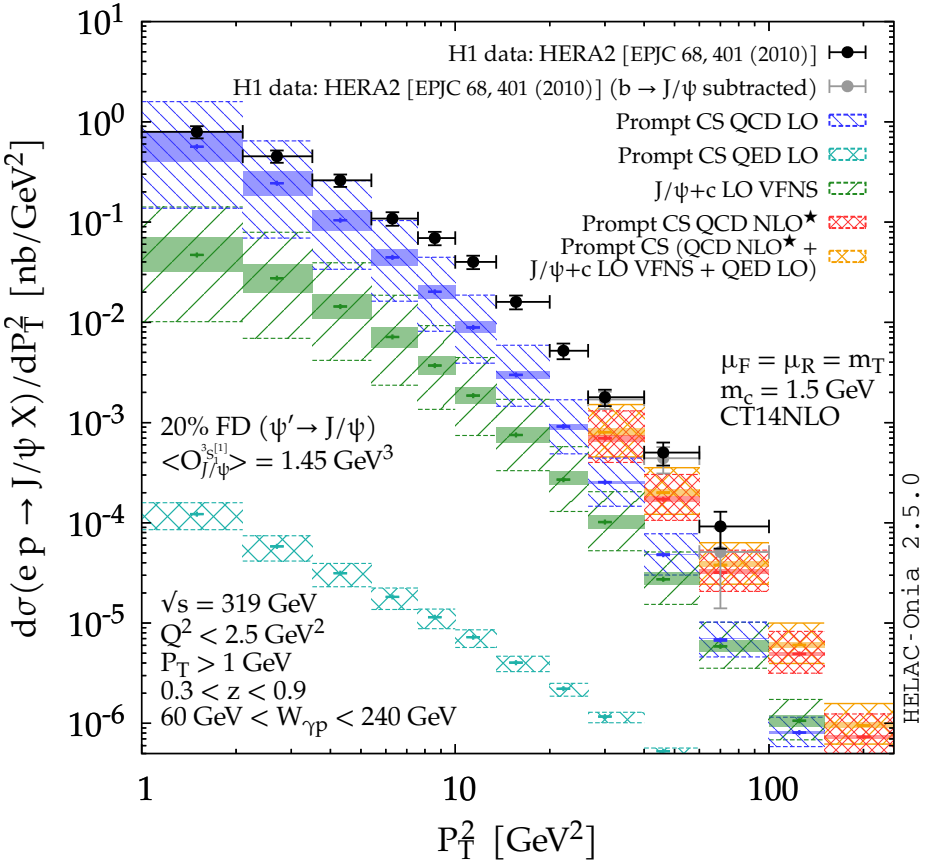

CF, J.-P. Lansberg, H.-S. Shao, Y. Yedelkina, PLB 811 (2020) 135926

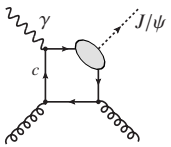

$\gamma + g \to \psi + g \,@\, \alpha\alpha_s^2$

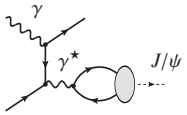

$\gamma + q \to \psi + q \,@\, \alpha^3$ [NEW!]

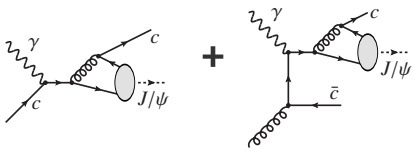

$$\begin{cases} \gamma+c\to\psi+c \,@\, \alpha\alpha_s^2 & \text{(4FS)} \\ \gamma+g\to\psi+c+\bar{c} \,@\, \alpha\alpha_s^3 & \text{(3FS)} \end{cases}$$ [also NEW!]

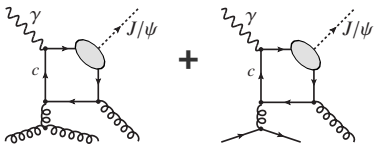

$$\begin{cases} \gamma+g\to\psi+g+g \,@\, \alpha\alpha_s^3 \\ \gamma+q\to\psi+g+q \,@\, \alpha\alpha_s^3 \end{cases}$$

[+ $\gamma + g \to \psi + g$]

All the computations are done with HELAC-ONIA [H.-S. Shao, CPC198 (2016) 238]. See also `https://nloaccess.in2p3.fr`
Scale and mass uncertainties are shown by the hatched and solid bands respectively.

[The quark and antiquark attached to the ellipsis are taken as on-shell and their relative velocity v is set to zero.]

Revisiting HERA data (II)

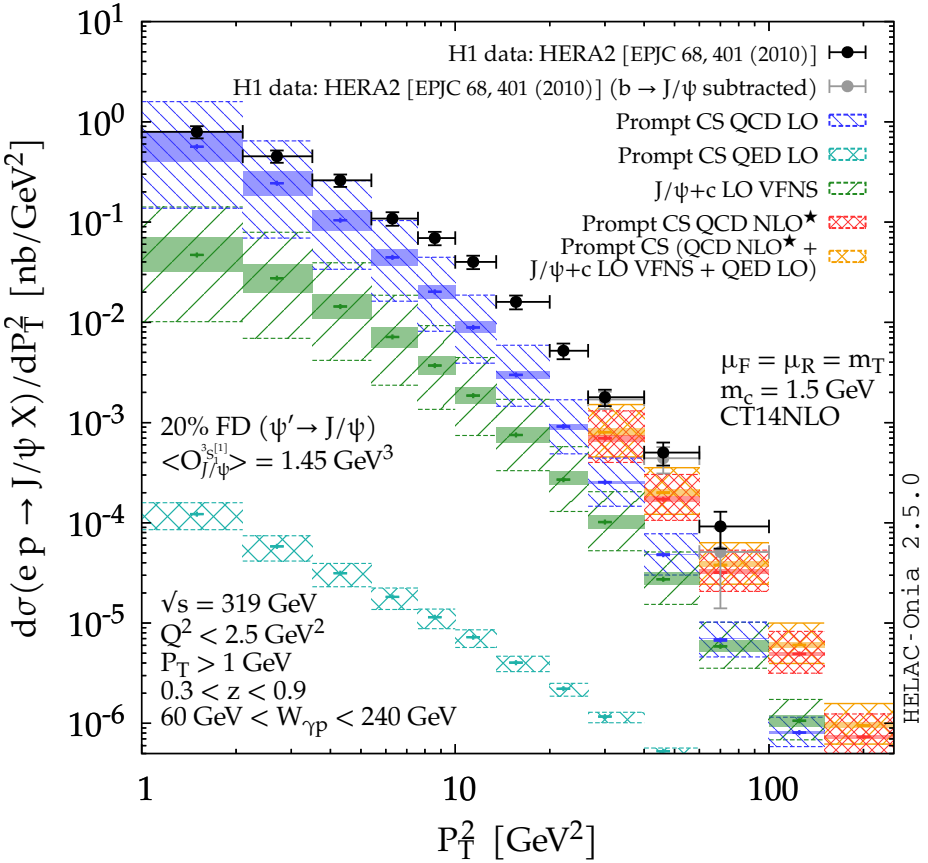

CF, J.-P. Lansberg, H.-S. Shao, Y. Yedelkina, PLB 811 (2020) 135926

- LO QCD works well at low P_T

Revisiting HERA data (II)

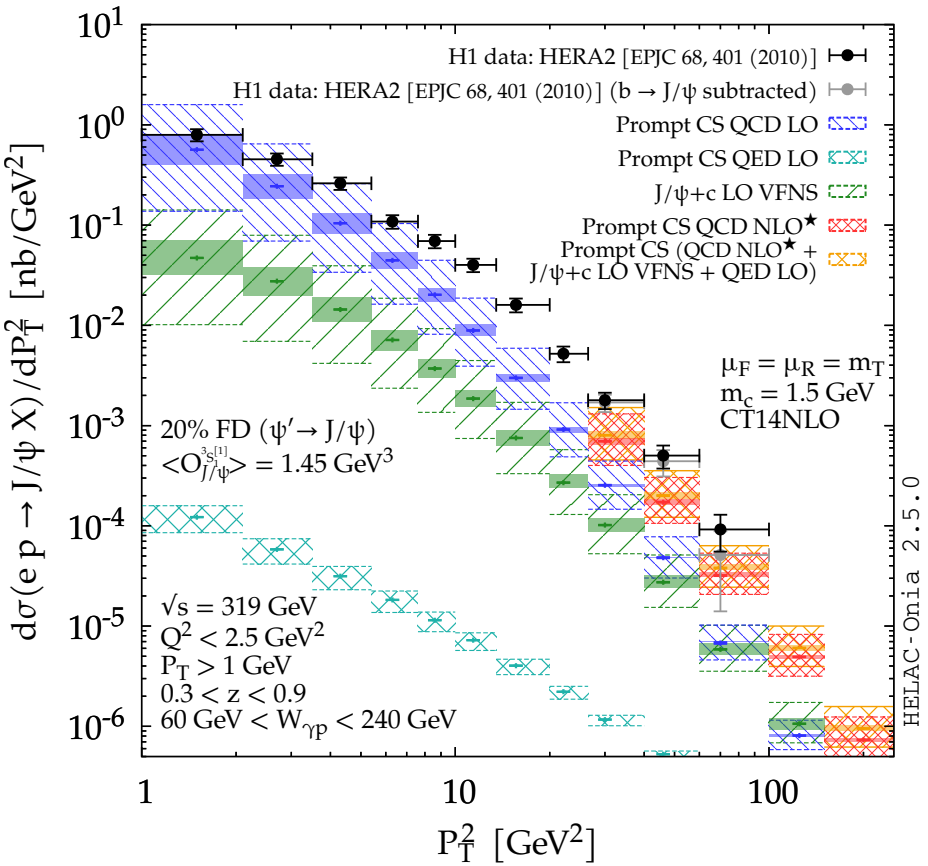

CF, J.-P. Lansberg, H.-S. Shao, Y. Yedelkina, PLB 811 (2020) 135926

- LO QCD works well at low P_T
- LO QED small, but much harder spectrum

Revisiting HERA data (II)

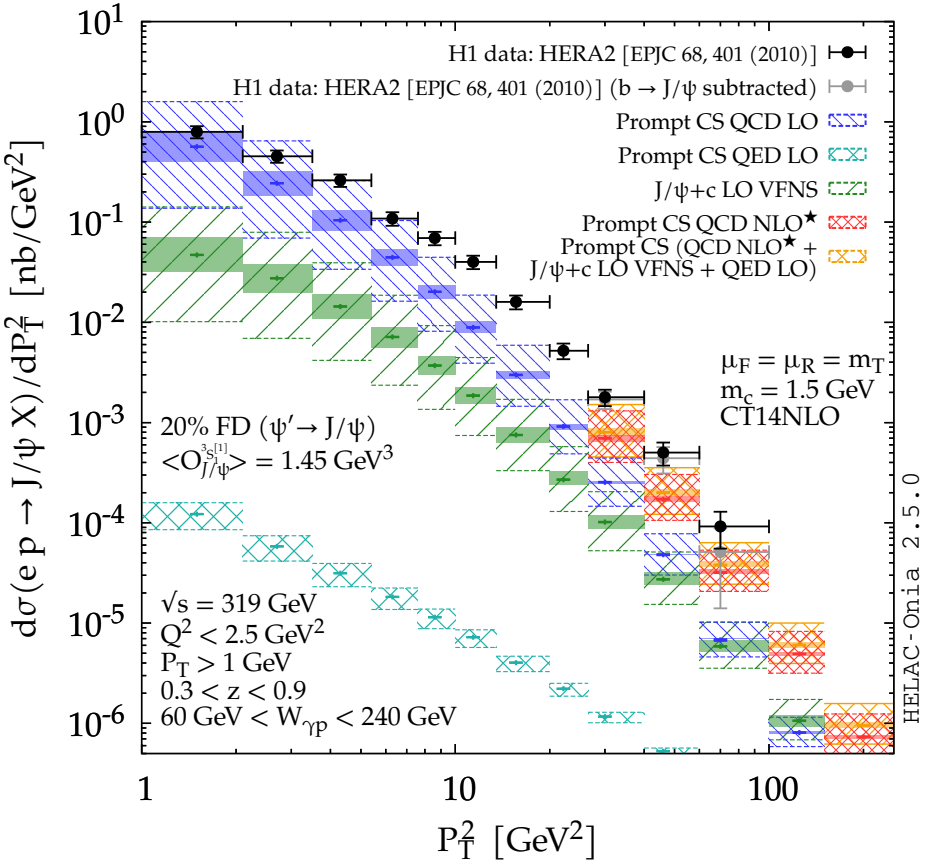

CF, J.-P. Lansberg, H.-S. Shao, Y. Yedelkina, PLB 811 (2020) 135926

- LO QCD works well at low P_T
- LO QED small, but much harder spectrum
- J/ψ+charm matters at large P_T

Revisiting HERA data (II)

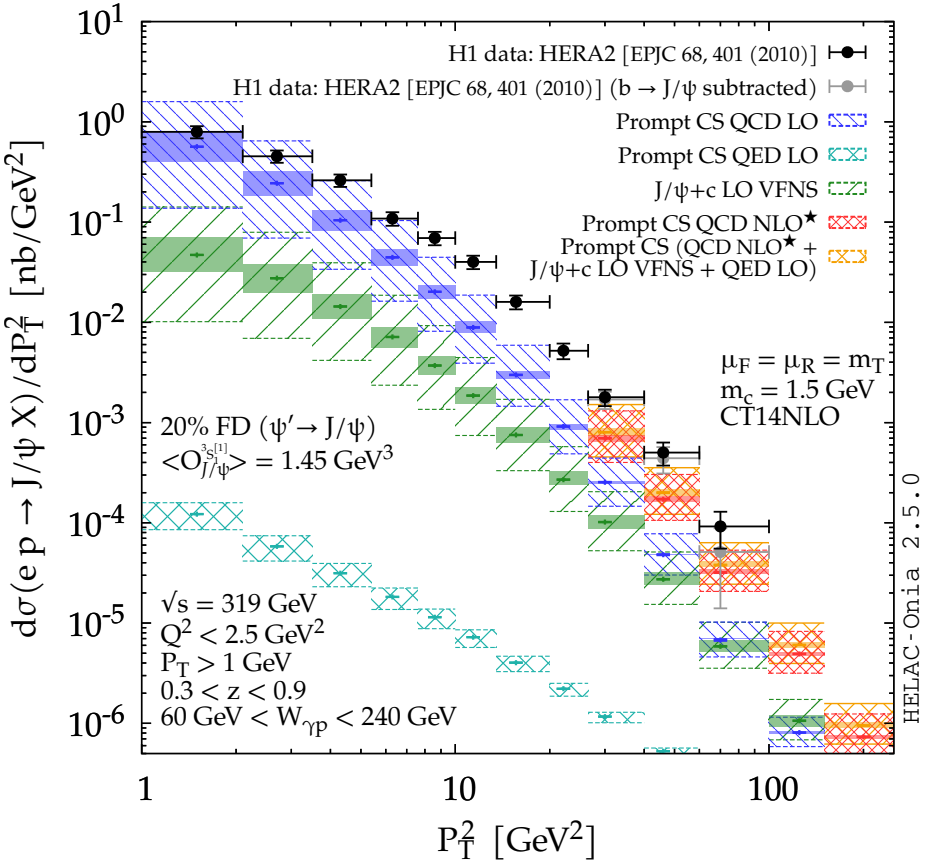

CF, J.-P. Lansberg, H.-S. Shao, Y. Yedelkina, PLB 811 (2020) 135926

- LO QCD works well at low P_T
- LO QED small, but much harder spectrum
- J/ψ+charm matters at large P_T
- NLO$^{(\star)}$ close to the data, the overall sum nearly agrees with them

Revisiting HERA data (II)

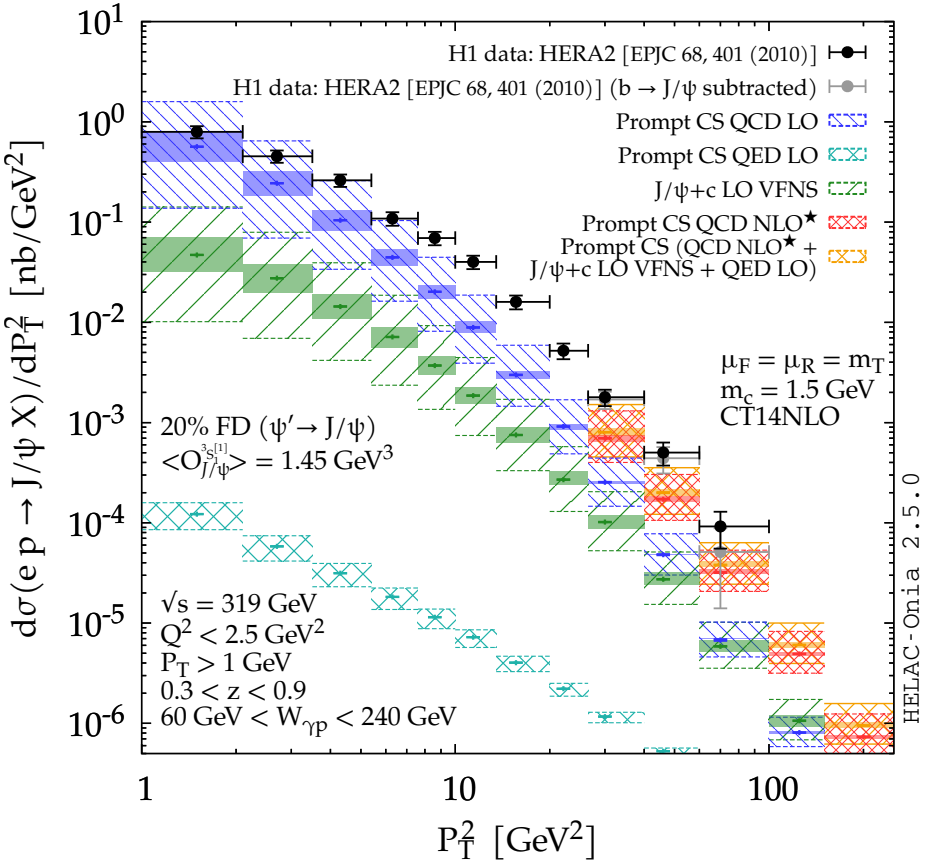

CF, J.-P. Lansberg, H.-S. Shao, Y. Yedelkina, PLB 811 (2020) 135926

- LO QCD works well at low P_T
- LO QED small, but much harder spectrum
- J/ψ+charm matters at large P_T
- NLO$^{(\star)}$ close to the data, the overall sum nearly agrees with them
- Agreement with the last bin when the expected $b \to J/\psi$ feed down A (in gray) is subtracted

Revisiting HERA data (II)

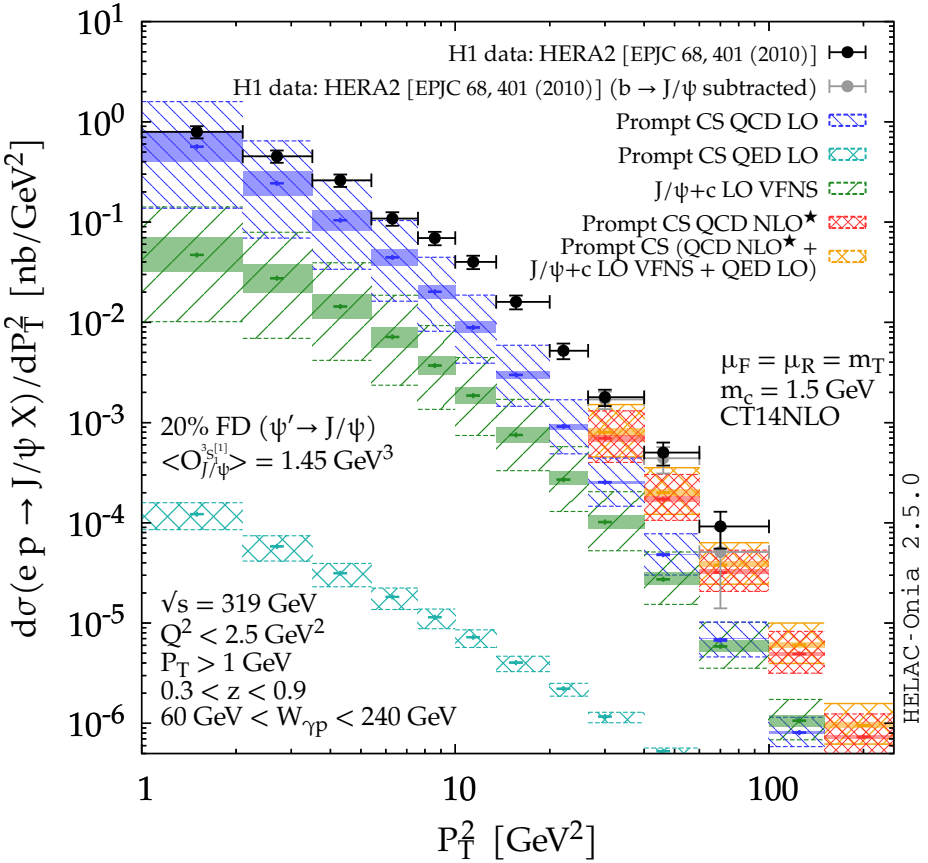

CF, J.-P. Lansberg, H.-S. Shao, Y. Yedelkina, PLB 811 (2020) 135926

- LO QCD works well at low P_T
- LO QED small, but much harder spectrum
- J/ψ+charm matters at large P_T
- NLO$^{(\star)}$ close to the data, the overall sum nearly agrees with them
- Agreement with the last bin when the expected $b \to J/\psi$ feed down A (in gray) is subtracted

The CSM up to $\alpha\alpha_s^3$ reproduces J/ψ photoproduction at HERA

$\to$ we will restrict to CSM for our EIC predictions

$J/\psi + X$ at the EIC

$[\sqrt{s_{ep}} = 45\ \text{GeV}]$

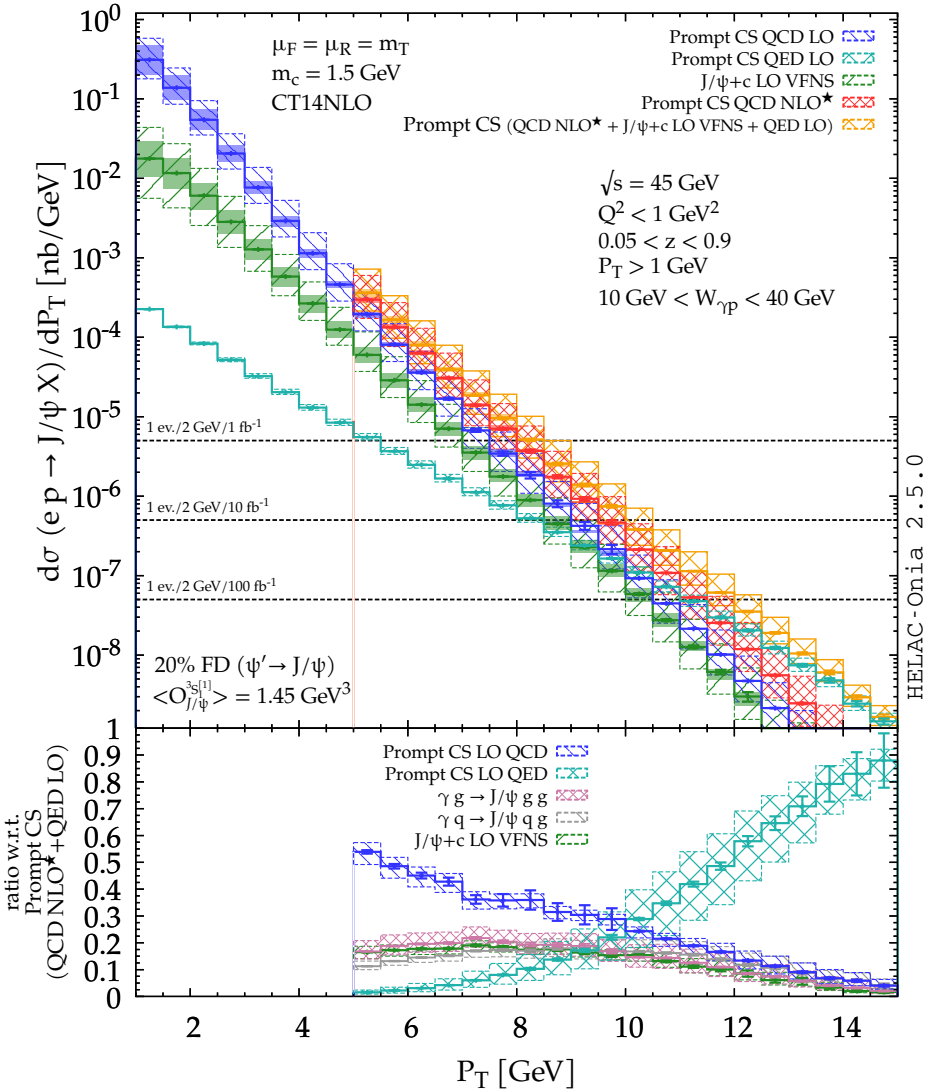

CF, J.-P. Lansberg, H.-S. Shao, Y. Yedelkina, PLB 811 (2020) 135926

- At $\sqrt{s_{ep}} = 45$ GeV, one gets into valence region

$J/\psi + X$ at the EIC

$[\sqrt{s_{ep}} = 45\ \text{GeV}]$

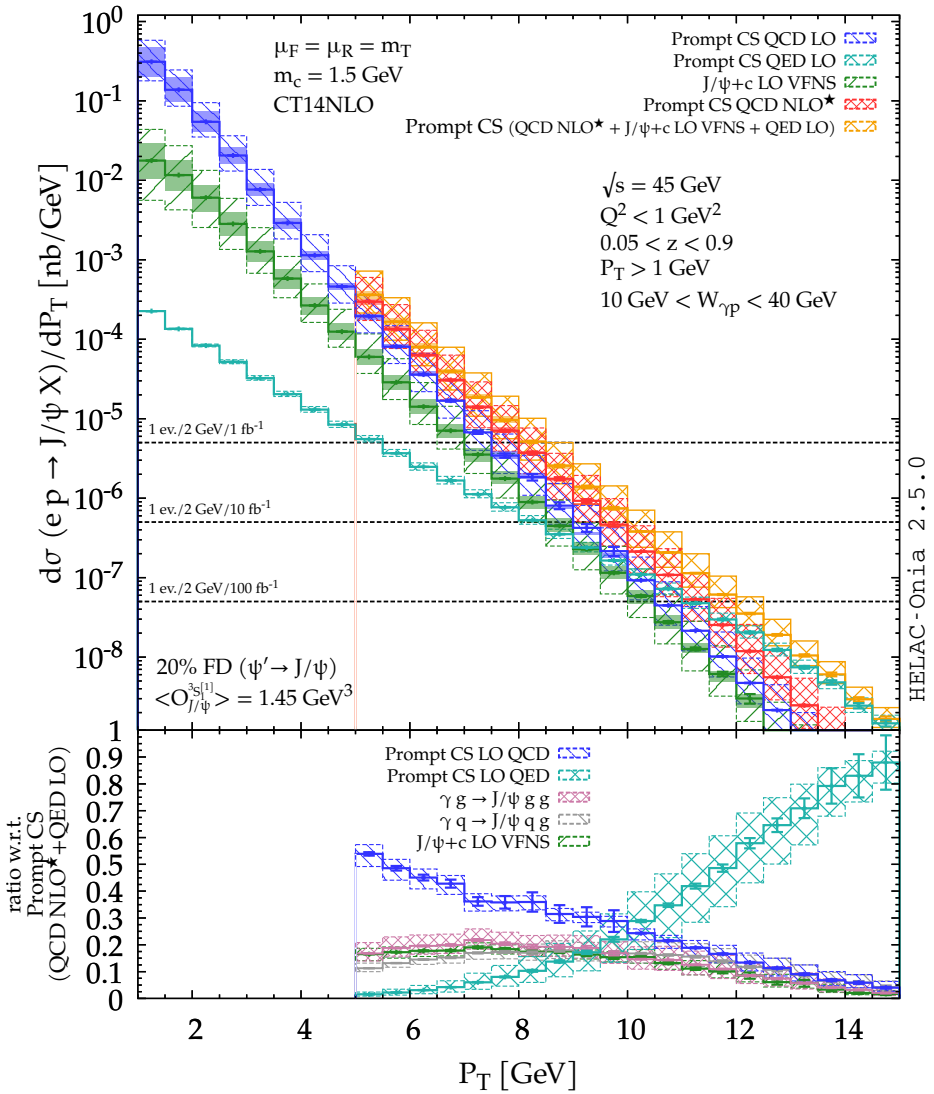

CF, J.-P. Lansberg, H.-S. Shao, Y. Yedelkina, PLB 811 (2020) 135926

- At $\sqrt{s_{ep}} = 45$ GeV, one gets into valence region
- Yield steeply falling with P_T
- Yield can be measured up to $P_T \sim 11$ GeV with $\mathcal{L} = 100$ fb^{-1}

[using both *ee* and $\mu\mu$ decay channels and $\varepsilon_{J/\psi} \simeq 80\%$]

$J/\psi + X$ at the EIC

$[\sqrt{s_{ep}} = 45\ \text{GeV}]$

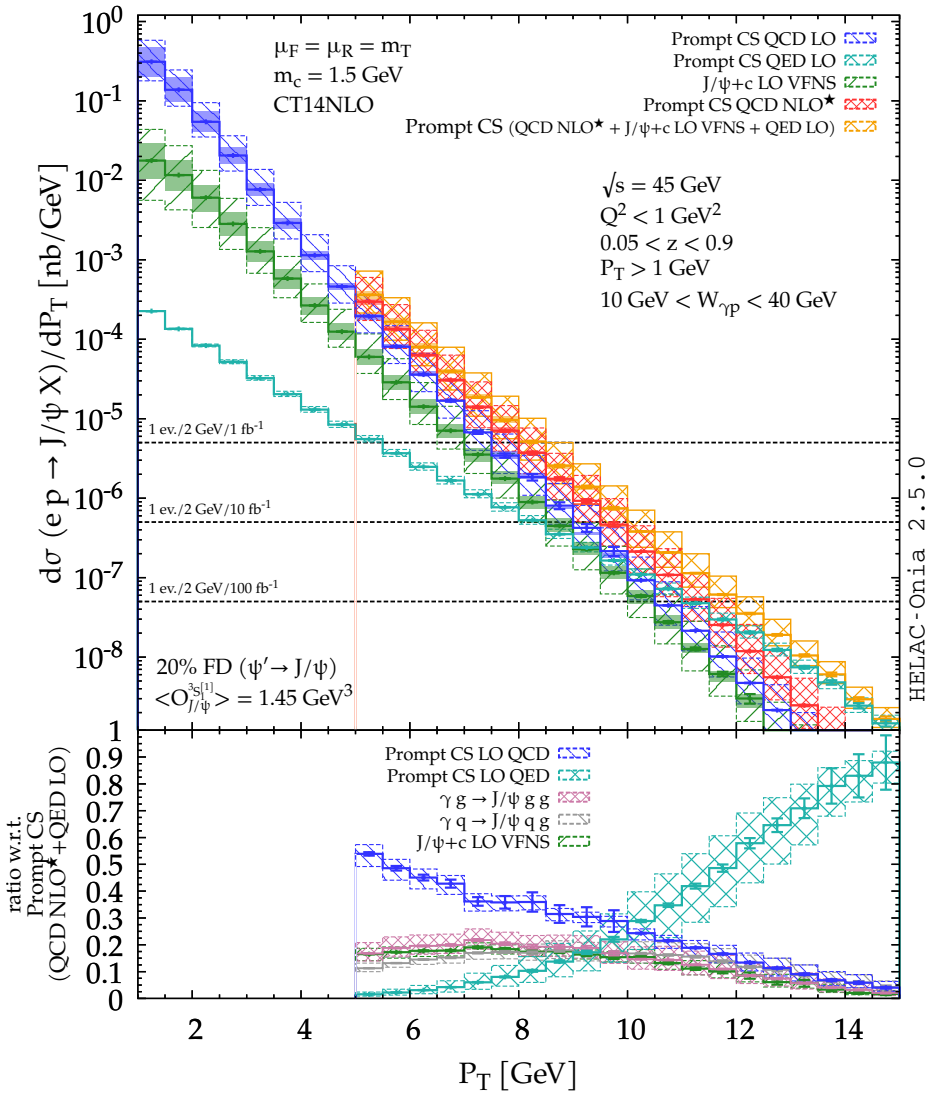

CF, J.-P. Lansberg, H.-S. Shao, Y. Yedelkina, PLB 811 (2020) 135926

- At $\sqrt{s_{ep}} = 45$ GeV, one gets into valence region
- Yield steeply falling with P_T
- Yield can be measured up to $P_T \sim 11$ GeV with $\mathcal{L} = 100$ fb^{-1}

  [using both *ee* and $\mu\mu$ decay channels and $\varepsilon_{J/\psi} \simeq 80\%$]
- QED contribution leading at the largest reachable P_T
- $\gamma + q$ fusion contributes more than 30% for $P_T > 8$ GeV

$J/\psi + X$ at the EIC

$\left[\sqrt{s_{ep}} = 140\ \text{GeV}\right]$

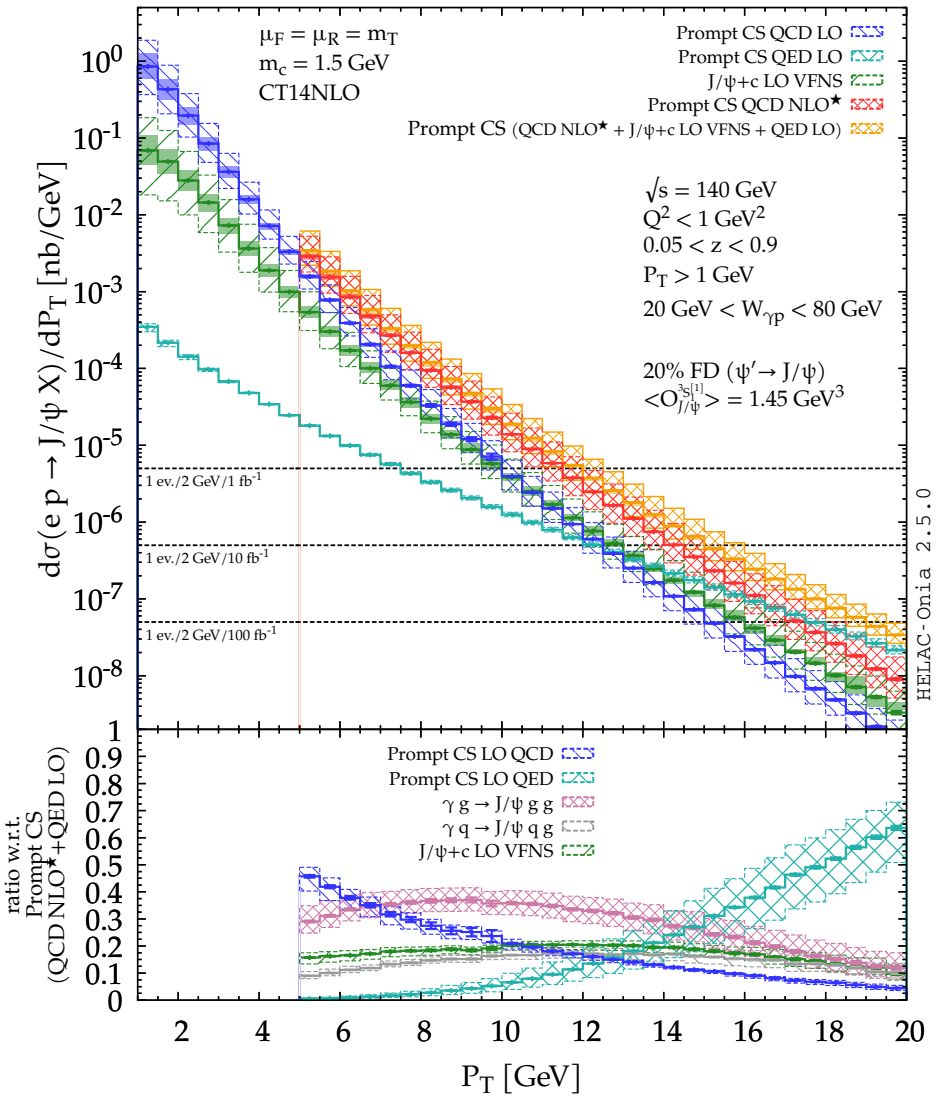

CF, J.-P. Lansberg, H.-S. Shao, Y. Yedelkina, PLB 811 (2020) 135926

- At $\sqrt{s_{ep}} = 140$ GeV larger P_T range, up to ~ 18 GeV

$J/\psi + X$ at the EIC

$\left[\sqrt{s_{ep}} = 140\ \text{GeV}\right]$

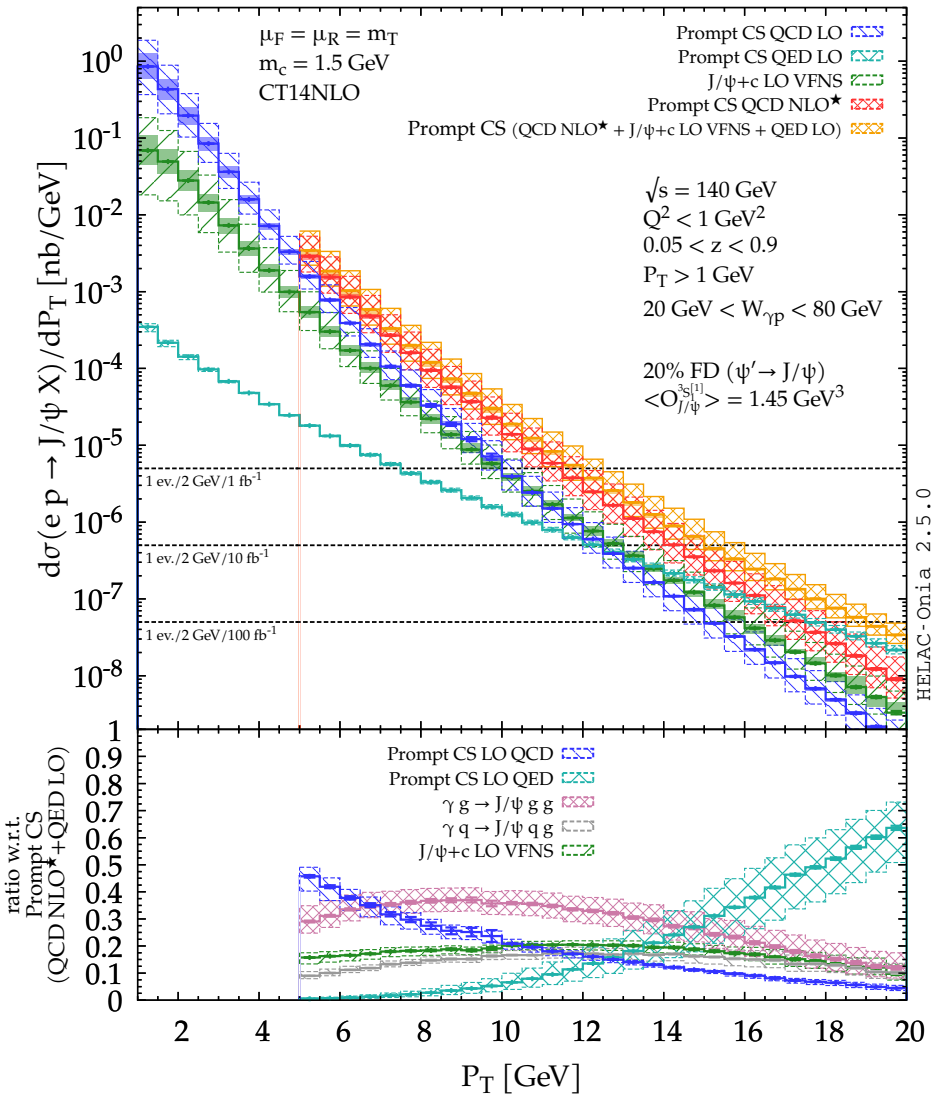

CF, J.-P. Lansberg, H.-S. Shao, Y. Yedelkina, PLB 811 (2020) 135926

- At $\sqrt{s_{ep}} = 140$ GeV larger P_T range, up to ~ 18 GeV
- QED contribution also leading at the largest reachable P_T
- $\gamma + g$ fusion contributions dominant up to $P_T \sim 15$ GeV

$J/\psi + X$ at the EIC

$[\sqrt{s_{ep}} = 140\ \text{GeV}]$

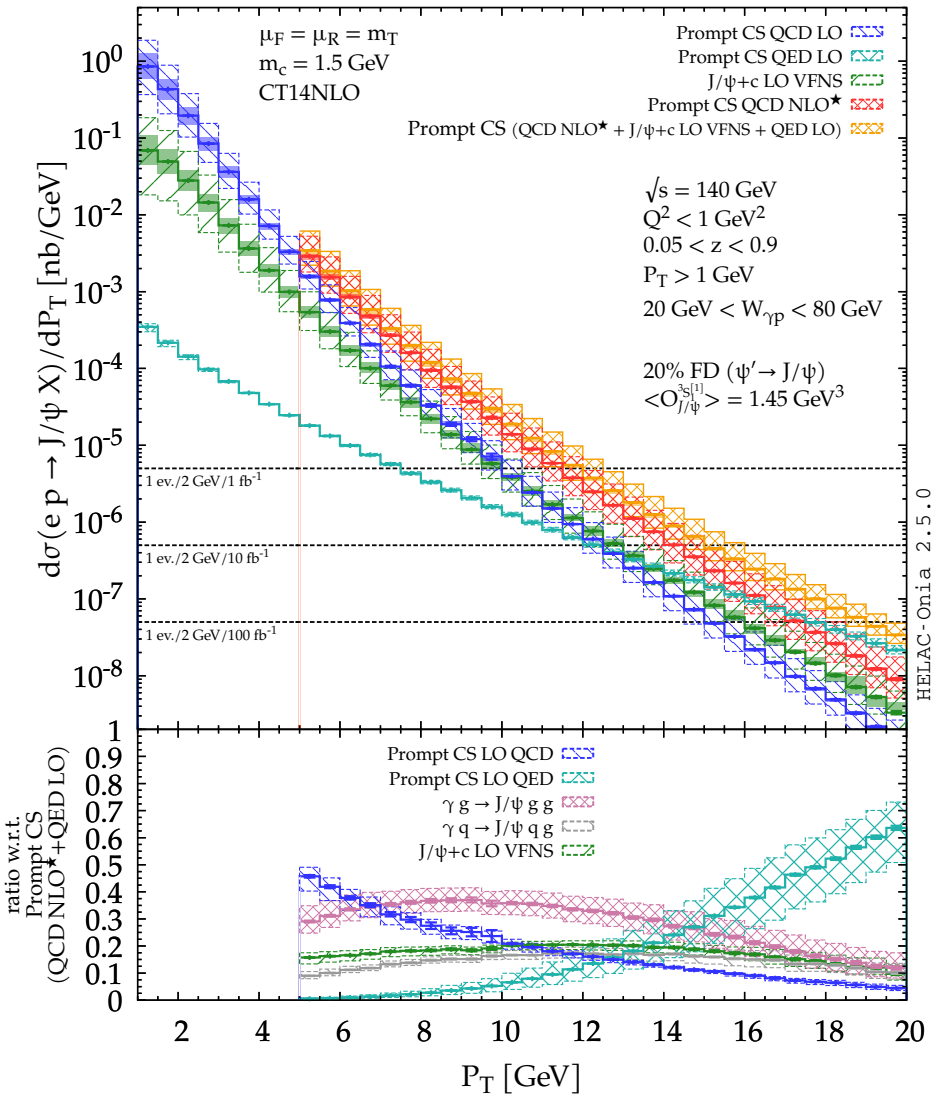

CF, J.-P. Lansberg, H.-S. Shao, Y. Yedelkina, PLB 811 (2020) 135926

- At $\sqrt{s_{ep}} = 140$ GeV larger P_T range, up to ~ 18 GeV
- QED contribution also leading at the largest reachable P_T
- $\gamma + g$ fusion contributions dominant up to $P_T \sim 15$ GeV
- $J/\psi + 2$ hard partons [*i.e.* $J/\psi + \{gg, qg, c\bar{c}\}$] dominant for $P_T \sim 8 - 15$ GeV

$J/\psi + X$ at the EIC

$[\sqrt{s_{ep}} = 140\ \text{GeV}]$

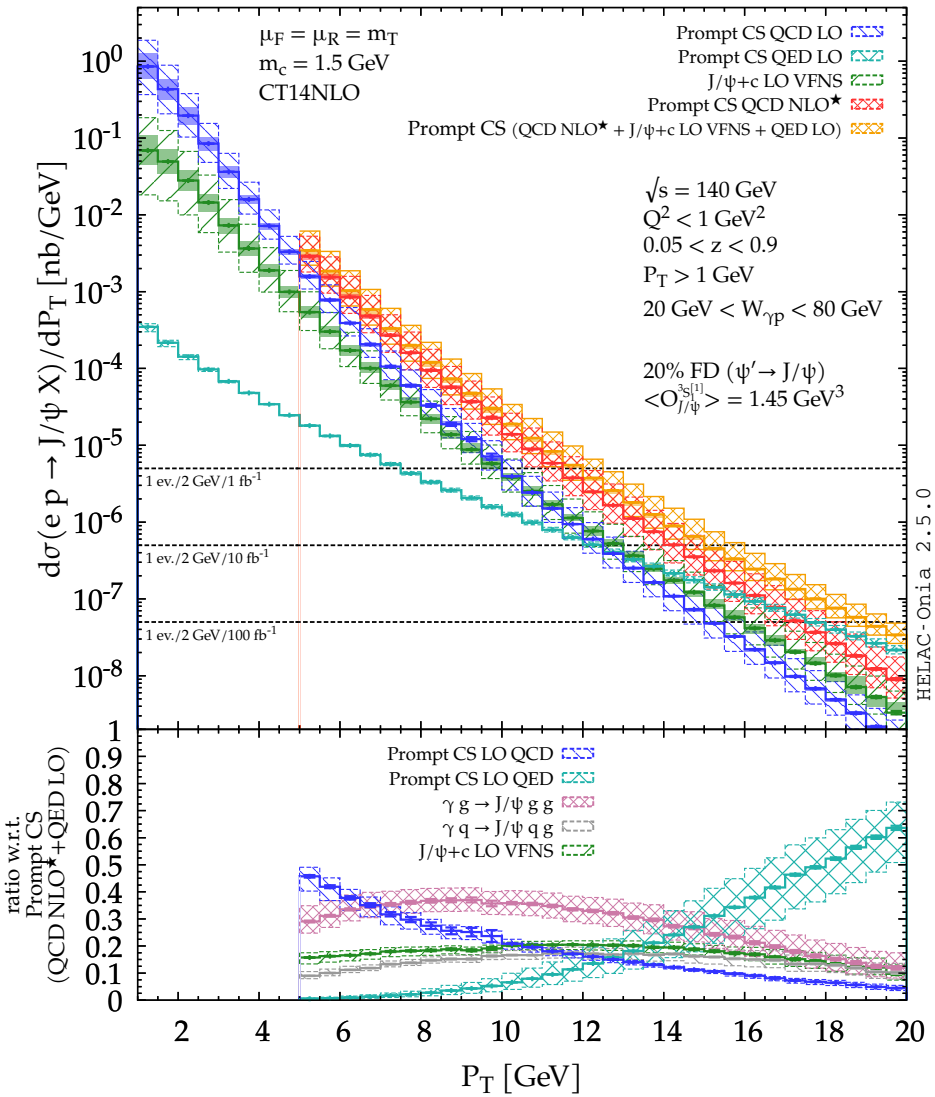

CF, J.-P. Lansberg, H.-S. Shao, Y. Yedelkina, PLB 811 (2020) 135926

- At $\sqrt{s_{ep}} = 140$ GeV larger P_T range, up to ~ 18 GeV
- QED contribution also leading at the largest reachable P_T
- $\gamma + g$ fusion contributions dominant up to $P_T \sim 15$ GeV
- $J/\psi + 2$ hard partons [*i.e.* $J/\psi + \{gg, qg, c\bar{c}\}$] dominant for $P_T \sim 8 - 15$ GeV
- It could lead to the observation of $J/\psi + 2$ jets with moderate P_T^{jet}

$J/\psi + X$ at the EIC

$\left[\sqrt{s_{ep}} = 140\ \text{GeV}\right]$

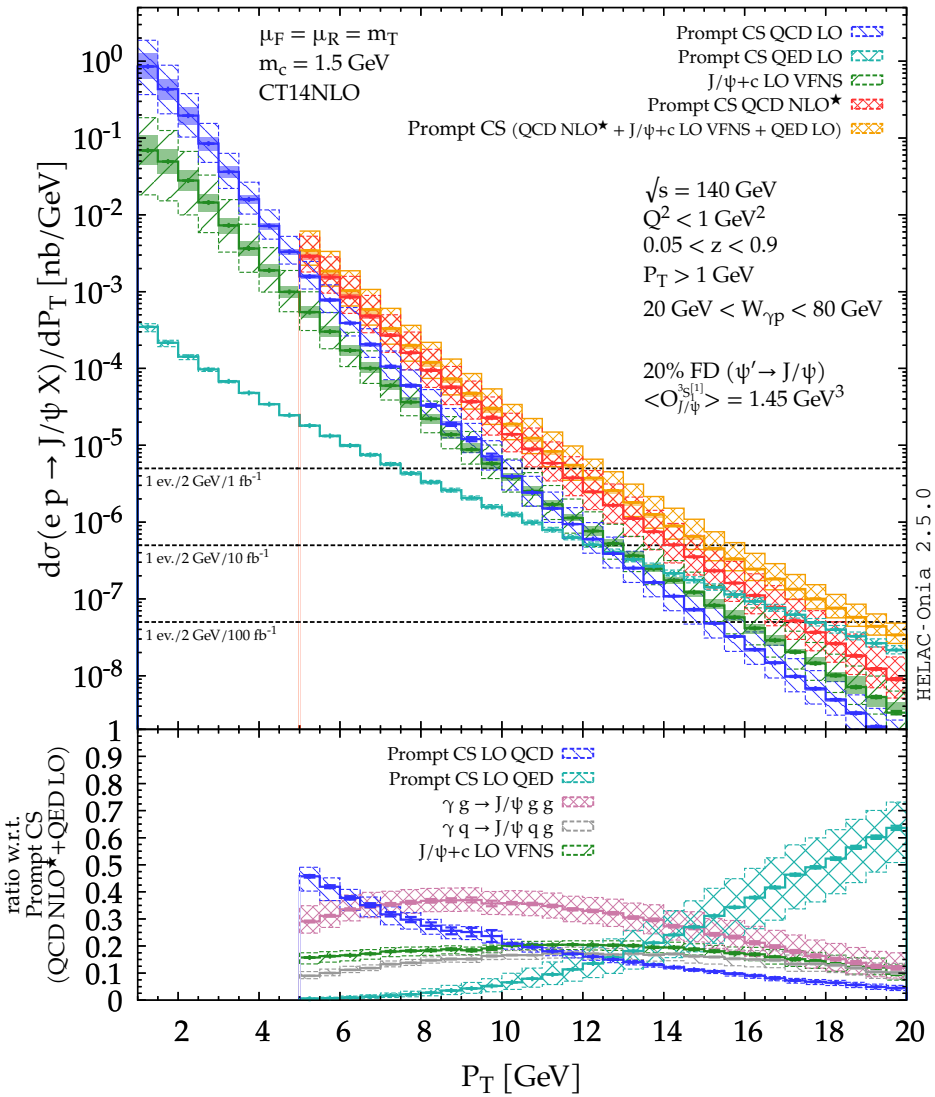

CF, J.-P. Lansberg, H.-S. Shao, Y. Yedelkina, PLB 811 (2020) 135926

- At $\sqrt{s_{ep}} = 140$ GeV larger P_T range, up to ~ 18 GeV
- QED contribution also leading at the largest reachable P_T
- $\gamma + g$ fusion contributions dominant up to $P_T \sim 15$ GeV
- $J/\psi + 2$ hard partons [*i.e.* $J/\psi + \{gg, qg, c\bar{c}\}$] dominant for $P_T \sim 8 - 15$ GeV
- It could lead to the observation of $J/\psi + 2$ jets with moderate P_T^{jet}
- with a specific topology where the leading jet$_1$ recoils on the J/ψ+ jet$_2$ pair

$J/\psi + X$ at the EIC

$\left[\sqrt{s_{ep}} = 140\ \text{GeV}\right]$

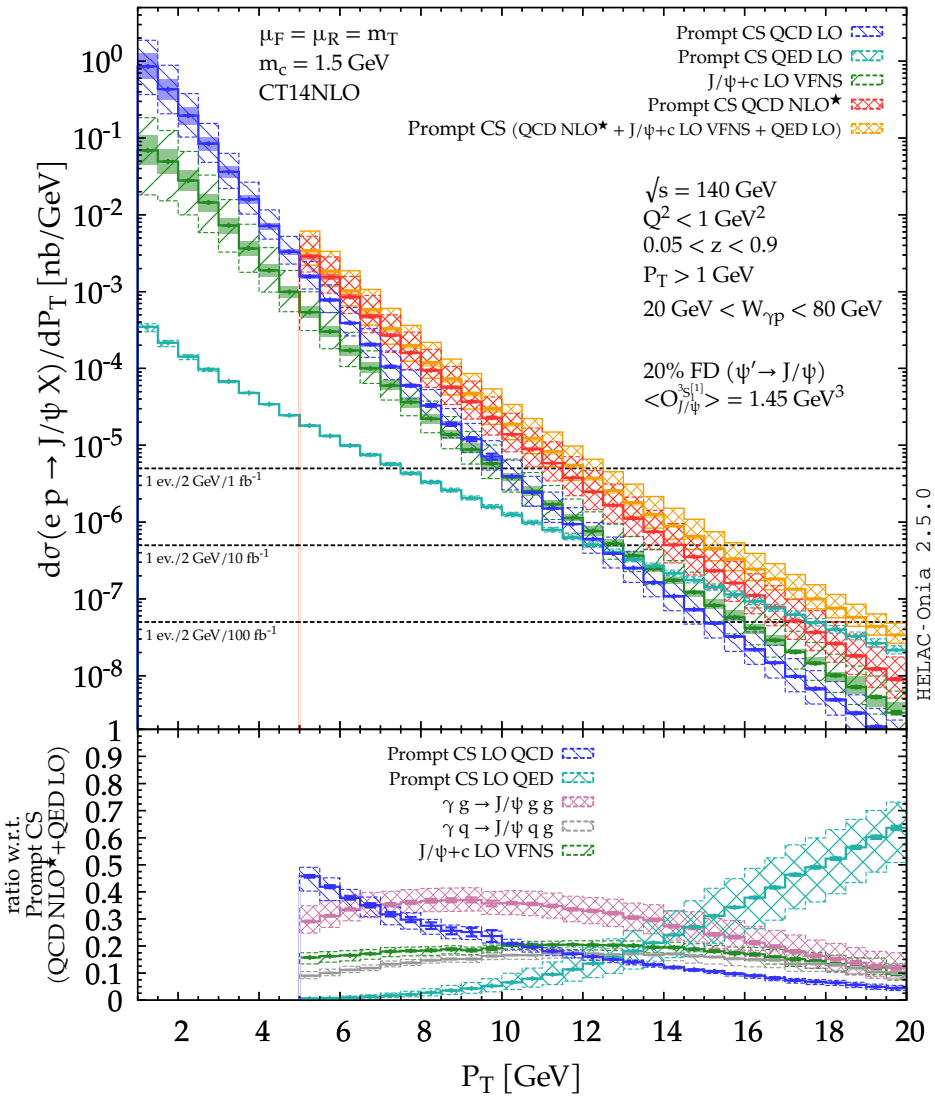

CF, J.-P. Lansberg, H.-S. Shao, Y. Yedelkina, PLB 811 (2020) 135926

- At $\sqrt{s_{ep}} = 140$ GeV larger P_T range, up to ~ 18 GeV
- QED contribution also leading at the largest reachable P_T
- $\gamma + g$ fusion contributions dominant up to $P_T \sim 15$ GeV
- $J/\psi + 2$ hard partons [*i.e.* $J/\psi + \{gg, qg, c\bar{c}\}$] dominant for $P_T \sim 8 - 15$ GeV
- It could lead to the observation of $J/\psi + 2$ jets with moderate P_T^{jet}
- with a specific topology where the leading jet$_1$ recoils on the J/ψ+ jet$_2$ pair
- We expect the $d\sigma$ to vanish when $E^{J/\psi \text{ rest fr.}}_{\text{jet}_2} \to 0$

J/ψ+charm associated production at the EIC

CF, J.-P. Lansberg, H.-S. Shao, Y. Yedelkina, PLB 811 (2020) 135926

J/ψ+charm associated production at the EIC

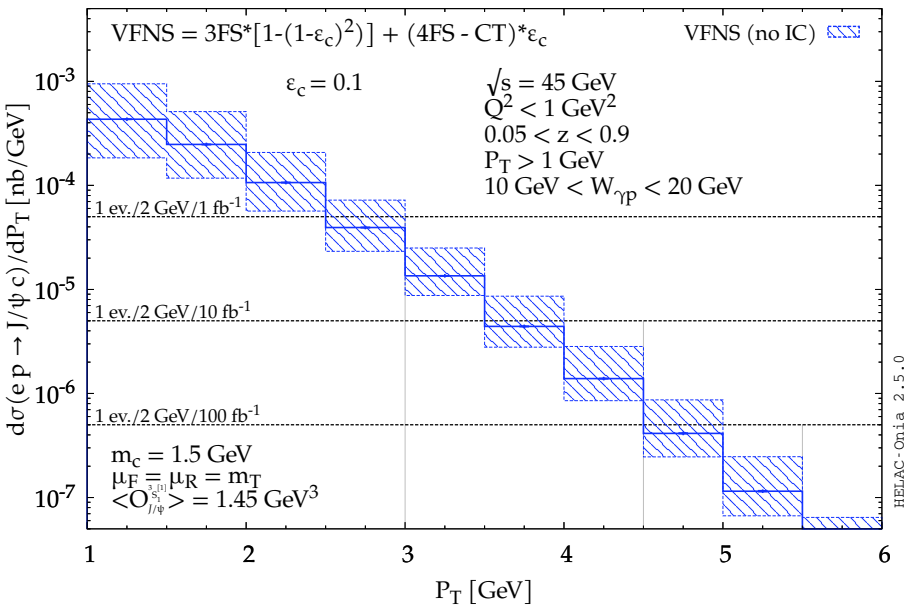

CF, J.-P. Lansberg, H.-S. Shao, Y. Yedelkina, PLB 811 (2020) 135926

- Same LO VFNS computation previously shown in green except for the charm-detection efficiency ε_c:

$$d\sigma^{\text{VFNS}} = d\sigma^{\text{3FS}}\left[1-(1-\varepsilon_c)^2\right] + \left(d\sigma^{\text{4FS}} - d\sigma^{\text{CT}}\right)\varepsilon_c$$

- At $\sqrt{s_{ep}} = 45$ GeV, yield limited to low P_T even with $\mathcal{L} = 100$ fb^{-1}
- But it is clearly observable if $\varepsilon_c = 0.1$ with $\mathcal{O}(500, 50, 5)$ events for $\mathcal{L} = (100, 10, 1)$ fb^{-1}

J/ψ+charm associated production at the EIC

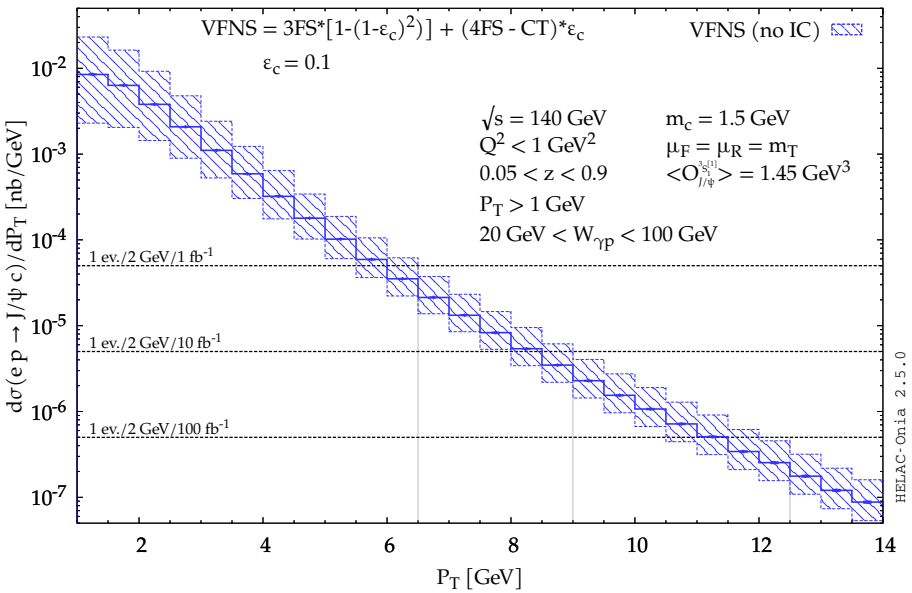

CF, J.-P. Lansberg, H.-S. Shao, Y. Yedelkina, PLB 811 (2020) 135926

- Same LO VFNS computation previously shown in green except for the charm-detection efficiency ε_c:

$$d\sigma^{\text{VFNS}} = d\sigma^{\text{3FS}}\left[1-(1-\varepsilon_c)^2\right] + \left(d\sigma^{\text{4FS}} - d\sigma^{\text{CT}}\right)\varepsilon_c$$

- At $\sqrt{s_{ep}} = 45$ GeV, yield limited to low P_T even with $\mathcal{L} = 100$ fb^{-1}
- But it is clearly observable if $\varepsilon_c = 0.1$ with $\mathcal{O}(500, 50, 5)$ events for $\mathcal{L} = (100, 10, 1)$ fb^{-1}
- At $\sqrt{s_{ep}} = 140$ GeV, P_T range up to 10 GeV with up to thousands of events with $\mathcal{L} = 100$ fb^{-1}
- Could be observed via charm jet

J/ψ+charm associated production at the EIC

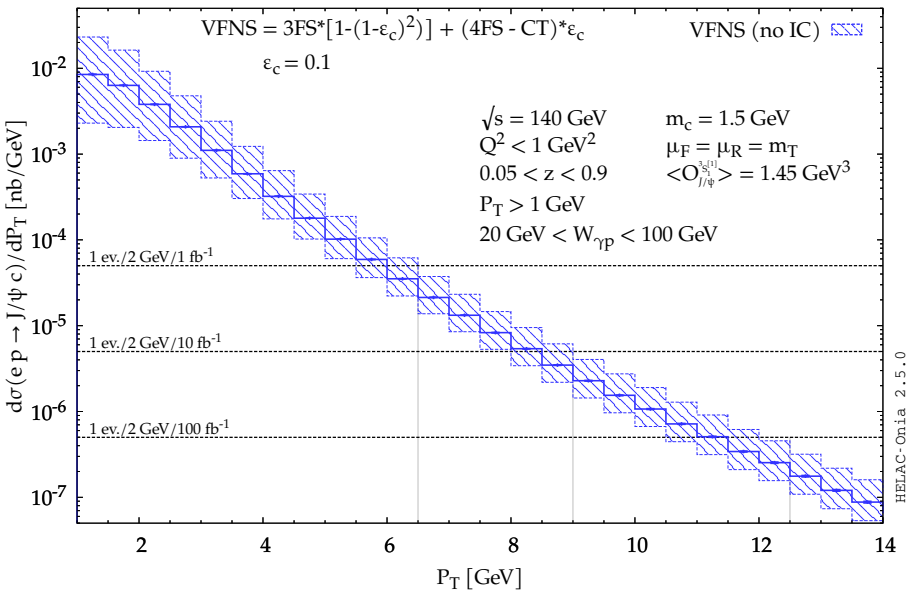

CF, J.-P. Lansberg, H.-S. Shao, Y. Yedelkina, PLB 811 (2020) 135926

- Same LO VFNS computation previously shown in green except for the charm-detection efficiency ε_c:

$$d\sigma^{\text{VFNS}} = d\sigma^{\text{3FS}}\left[1-(1-\varepsilon_c)^2\right] + \left(d\sigma^{\text{4FS}} - d\sigma^{\text{CT}}\right)\varepsilon_c$$

- At $\sqrt{s_{ep}} = 45$ GeV, yield limited to low P_T even with $\mathcal{L} = 100$ fb^{-1}
- But it is clearly observable if $\varepsilon_c = 0.1$ with $\mathcal{O}(500, 50, 5)$ events for $\mathcal{L} = (100, 10, 1)$ fb^{-1}
- At $\sqrt{s_{ep}} = 140$ GeV, P_T range up to 10 GeV with up to thousands of events with $\mathcal{L} = 100$ fb^{-1}
- Could be observed via charm jet

- 4FS $\gamma c \to J/\psi c$ depends on $c(x)$ and could be enhanced by intrinsic charm

J/ψ+charm associated production at the EIC

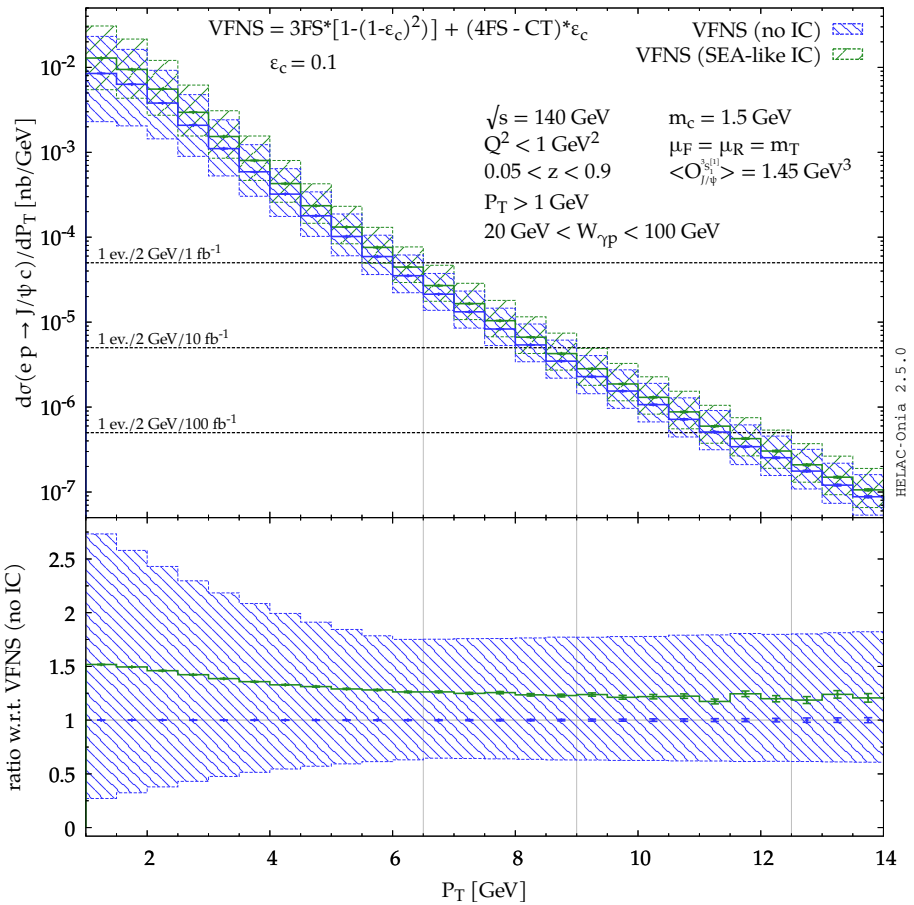

CF, J.-P. Lansberg, H.-S. Shao, Y. Yedelkina, PLB 811 (2020) 135926

- Same LO VFNS computation previously shown in green except for the charm-detection efficiency ε_c:

$$d\sigma^{\text{VFNS}} = d\sigma^{\text{3FS}}\left[1-(1-\varepsilon_c)^2\right] + \left(d\sigma^{\text{4FS}} - d\sigma^{\text{CT}}\right)\varepsilon_c$$

- At $\sqrt{s_{ep}} = 45$ GeV, yield limited to low P_T even with $\mathcal{L} = 100$ fb^{-1}
- But it is clearly observable if $\varepsilon_c = 0.1$ with $\mathcal{O}(500, 50, 5)$ events for $\mathcal{L} = (100, 10, 1)$ fb^{-1}
- At $\sqrt{s_{ep}} = 140$ GeV, P_T range up to 10 GeV with up to thousands of events with $\mathcal{L} = 100$ fb^{-1}
- Could be observed via charm jet

- 4FS $\gamma c \to J/\psi c$ depends on $c(x)$ and could be enhanced by intrinsic charm
- Small effect at $\sqrt{s_{ep}} = 140$ GeV

[We used IC $c(x)$ encoded in CT14NNLO]

J/ψ+charm associated production at the EIC

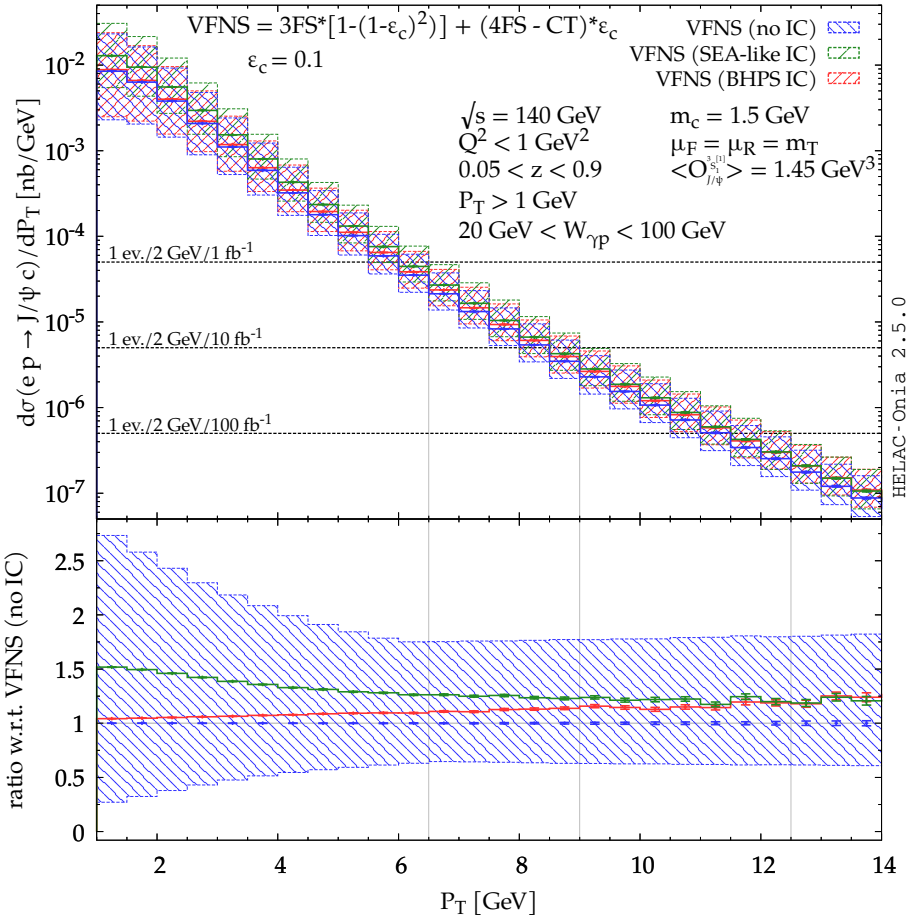

CF, J.-P. Lansberg, H.-S. Shao, Y. Yedelkina, PLB 811 (2020) 135926

- Same LO VFNS computation previously shown in green except for the charm-detection efficiency ε_c:

$$d\sigma^{\text{VFNS}} = d\sigma^{\text{3FS}}\left[1-(1-\varepsilon_c)^2\right] + \left(d\sigma^{\text{4FS}} - d\sigma^{\text{CT}}\right)\varepsilon_c$$

- At $\sqrt{s_{ep}} = 45$ GeV, yield limited to low P_T even with $\mathcal{L} = 100$ fb^{-1}
- But it is clearly observable if $\varepsilon_c = 0.1$ with $\mathcal{O}(500, 50, 5)$ events for $\mathcal{L} = (100, 10, 1)$ fb^{-1}
- At $\sqrt{s_{ep}} = 140$ GeV, P_T range up to 10 GeV with up to thousands of events with $\mathcal{L} = 100$ fb^{-1}
- Could be observed via charm jet

- 4FS $\gamma c \to J/\psi c$ depends on $c(x)$ and could be enhanced by intrinsic charm
- Small effect at $\sqrt{s_{ep}} = 140$ GeV

[We used IC $c(x)$ encoded in CT14NNLO]

J/ψ+charm associated production at the EIC

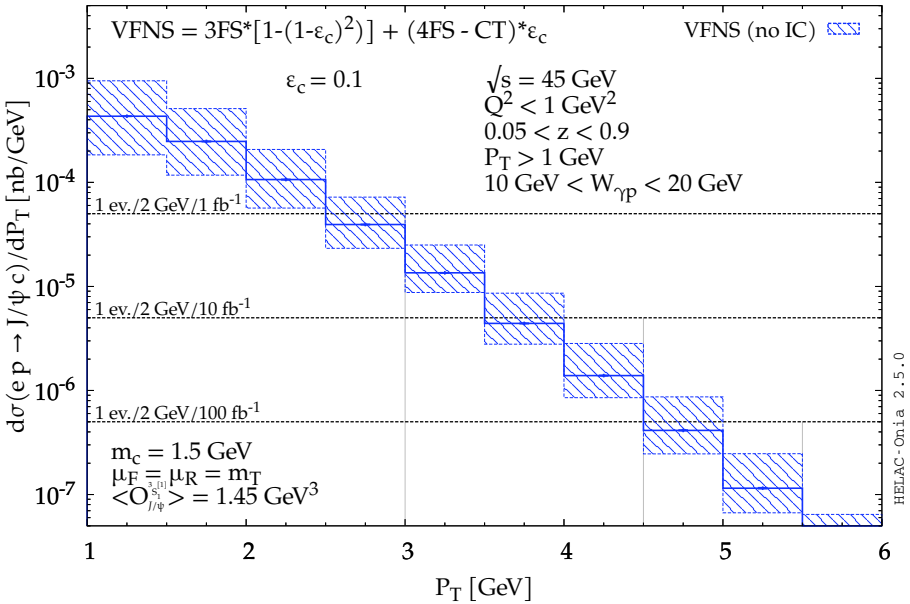

CF, J.-P. Lansberg, H.-S. Shao, Y. Yedelkina, PLB 811 (2020) 135926

- Same LO VFNS computation previously shown in green except for the charm-detection efficiency ε_c:

$$d\sigma^{\text{VFNS}} = d\sigma^{\text{3FS}}\left[1-(1-\varepsilon_c)^2\right] + \left(d\sigma^{\text{4FS}} - d\sigma^{\text{CT}}\right)\varepsilon_c$$

- At $\sqrt{s_{ep}} = 45$ GeV, yield limited to low P_T even with $\mathcal{L} = 100$ fb^{-1}
- But it is clearly observable if $\varepsilon_c = 0.1$ with $\mathcal{O}(500, 50, 5)$ events for $\mathcal{L} = (100, 10, 1)$ fb^{-1}
- At $\sqrt{s_{ep}} = 140$ GeV, P_T range up to 10 GeV with up to thousands of events with $\mathcal{L} = 100$ fb^{-1}
- Could be observed via charm jet

- 4FS $\gamma c \to J/\psi c$ depends on $c(x)$ and could be enhanced by intrinsic charm
- Small effect at $\sqrt{s_{ep}} = 140$ GeV
- Measurable effect at $\sqrt{s_{ep}} = 45$ GeV

[We used IC $c(x)$ encoded in CT14NNLO]

J/ψ+charm associated production at the EIC

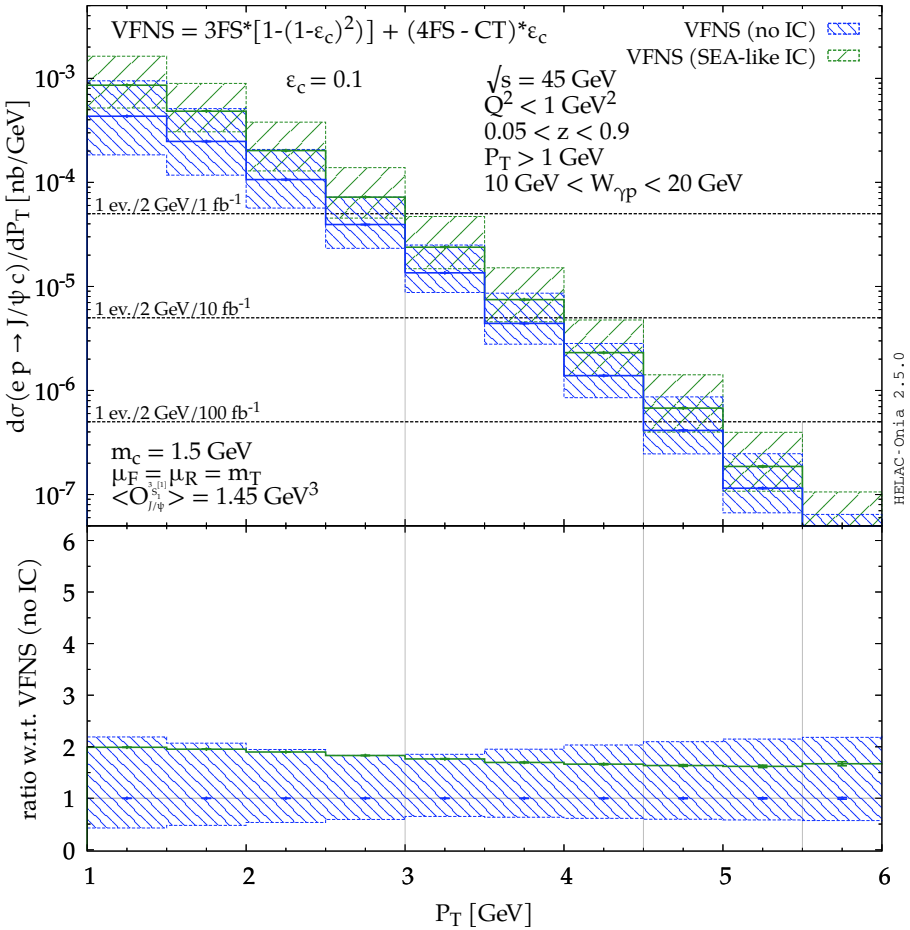

CF, J.-P. Lansberg, H.-S. Shao, Y. Yedelkina, PLB 811 (2020) 135926

- Same LO VFNS computation previously shown in green except for the charm-detection efficiency ε_c:

$$d\sigma^{\text{VFNS}} = d\sigma^{\text{3FS}}\left[1-(1-\varepsilon_c)^2\right] + \left(d\sigma^{\text{4FS}} - d\sigma^{\text{CT}}\right)\varepsilon_c$$

- At $\sqrt{s_{ep}} = 45$ GeV, yield limited to low P_T even with $\mathcal{L} = 100$ fb^{-1}
- But it is clearly observable if $\varepsilon_c = 0.1$ with $\mathcal{O}(500, 50, 5)$ events for $\mathcal{L} = (100, 10, 1)$ fb^{-1}
- At $\sqrt{s_{ep}} = 140$ GeV, P_T range up to 10 GeV with up to thousands of events with $\mathcal{L} = 100$ fb^{-1}
- Could be observed via charm jet

- 4FS $\gamma c \to J/\psi c$ depends on $c(x)$ and could be enhanced by intrinsic charm
- Small effect at $\sqrt{s_{ep}} = 140$ GeV
- Measurable effect at $\sqrt{s_{ep}} = 45$ GeV

[We used IC $c(x)$ encoded in CT14NNLO]

J/ψ+charm associated production at the EIC

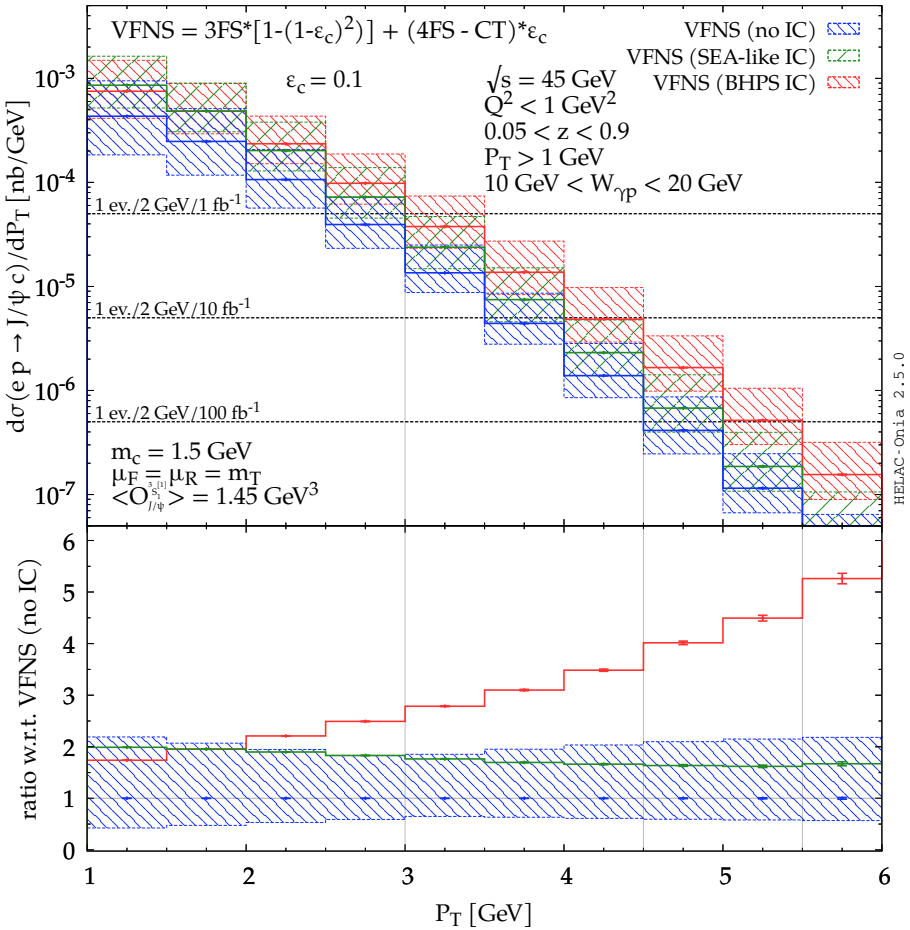

CF, J.-P. Lansberg, H.-S. Shao, Y. Yedelkina, PLB 811 (2020) 135926

- Same LO VFNS computation previously shown in green except for the charm-detection efficiency ε_c:

$$d\sigma^{\text{VFNS}} = d\sigma^{\text{3FS}}\left[1-(1-\varepsilon_c)^2\right] + \left(d\sigma^{\text{4FS}} - d\sigma^{\text{CT}}\right)\varepsilon_c$$

- At $\sqrt{s_{ep}} = 45$ GeV, yield limited to low P_T even with $\mathcal{L} = 100$ fb^{-1}
- But it is clearly observable if $\varepsilon_c = 0.1$ with $\mathcal{O}(500, 50, 5)$ events for $\mathcal{L} = (100, 10, 1)$ fb^{-1}
- At $\sqrt{s_{ep}} = 140$ GeV, P_T range up to 10 GeV with up to thousands of events with $\mathcal{L} = 100$ fb^{-1}
- Could be observed via charm jet

- 4FS $\gamma c \to J/\psi c$ depends on $c(x)$ and could be enhanced by intrinsic charm
- Small effect at $\sqrt{s_{ep}} = 140$ GeV
- Measurable effect at $\sqrt{s_{ep}} = 45$ GeV:

[We used IC $c(x)$ encoded in CT14NNLO]
BHPS valence-like peak visible!

Conclusions

Conclusions

- No agreement on the quarkonium-inclusive-production mechanisms

Conclusions

- No agreement on the quarkonium-inclusive-production mechanisms
- For quarkonium production, QCD corrections with P_T-enhanced topologies are known to be important

We have revisited J/ψ photoproduction at HERA

Conclusions

- No agreement on the quarkonium-inclusive-production mechanisms
- For quarkonium production, QCD corrections with P_T-enhanced topologies are known to be important

  We have revisited J/ψ photoproduction at HERA
- CSM can describe the latest HERA photoproduction data

  Agreement improved when accounting for J/ψ+charm and $b \to J/\psi$ FD contributions

Conclusions

- No agreement on the quarkonium-inclusive-production mechanisms
- For quarkonium production, QCD corrections with P_T-enhanced topologies are known to be important

  We have revisited J/ψ photoproduction at HERA
- CSM can describe the latest HERA photoproduction data

  Agreement improved when accounting for J/ψ+charm and $b \to J/\psi$ FD contributions
- We have presented the first QCD-correction study to inclusive J/ψ photoproduction at the EIC

  [for leptoproduction ($Q^2 \neq 0$): see **J.W. Qiu** *et al.* **2005.10832** or **S. Rajesh talk (today, 10:37, Spin Phys. WG)**]

Conclusions

- No agreement on the quarkonium-inclusive-production mechanisms
- For quarkonium production, QCD corrections with P_T-enhanced topologies are known to be important

  We have revisited J/ψ photoproduction at HERA
- CSM can describe the latest HERA photoproduction data

  Agreement improved when accounting for J/ψ+charm and $b \to J/\psi$ FD contributions
- We have presented the first QCD-correction study to inclusive J/ψ photoproduction at the EIC

  [for leptoproduction ($Q^2 \neq 0$): see **J.W. Qiu** *et al.* **2005.10832** or **S. Rajesh talk (today, 10:37, Spin Phys. WG)**]
- $\sqrt{s_{ep}} = 140$ GeV:
  - $\gamma + q$ QED contribution [new!] leading at large P_T
  - $\gamma + g$ fusion mostly dominant
  - J/ψ+charm jet accessible
  - $J/\psi + 2$ jets accessible

Conclusions

- No agreement on the quarkonium-inclusive-production mechanisms
- For quarkonium production, QCD corrections with P_T-enhanced topologies are known to be important

  We have revisited J/ψ photoproduction at HERA
- CSM can describe the latest HERA photoproduction data

  Agreement improved when accounting for J/ψ+charm and $b \to J/\psi$ FD contributions
- We have presented the first QCD-correction study to inclusive J/ψ photoproduction at the EIC

  [for leptoproduction ($Q^2 \neq 0$): see **J.W. Qiu** *et al.* **2005.10832** or **S. Rajesh talk (today, 10:37, Spin Phys. WG)**]
- $\sqrt{s_{ep}} = 140$ GeV:
  - $\gamma + q$ QED contribution [new!] leading at large P_T
  - $\gamma + g$ fusion mostly dominant
  - J/ψ+charm jet accessible
  - $J/\psi + 2$ jets accessible
- $\sqrt{s_{ep}} = 45$ GeV:
  - $\gamma + q$ QED contribution [new!] leading at high P_T
  - J/ψ+charm sensitive to charm PDFs

Thank you

Backup

Kinematics and cross section

CF, J.-P. Lansberg, H.-S. Shao, Y. Yedelkina, PLB 811 (2020) 135926

- $s_{ep} = (P_e + P_p)^2 = 4E_eE_p$; $s_{\gamma p} = W^2_{\gamma p} = (P_\gamma + P_p)^2$; $P_\gamma = x_\gamma P_e$, so $s_{\gamma p} = x_\gamma s_{ep}$
- $z = \frac{P_{\mathcal{Q}} \cdot P_p}{P_\gamma \cdot P_p}$: fraction of the photon energy taken by the J/ψ in the proton rest frame
- cross section:

$$\frac{d\sigma}{dz dP_T} = \int_{x_\gamma^{\min}}^1 dx_\gamma \frac{2x_a P_T f_{\gamma/e}(x_\gamma, Q^2_{\max}) f_{a/p}(x_a(x_\gamma), \mu_F)}{z(1-z)} \times \frac{1}{16\pi \hat{s}^2} \overline{|\mathcal{M}(\gamma + a \to \mathcal{Q} + k)|^2},$$

  where $x_a = \frac{M_T^2 - m_{\mathcal{Q}}^2 z}{x_\gamma s_{ep} z(1-z)}$ and $x_\gamma^{\min} = \frac{M_T^2 - m_{\mathcal{Q}}^2 z}{s_{ep} z(1-z)}$

- WW distribution

$$f_{\gamma/e}(x_\gamma, Q^2_{\max}) = \frac{\alpha}{2\pi}\left[\frac{1+(1-x_\gamma)^2}{x_\gamma} \ln \frac{Q^2_{\max}}{Q^2_{\min}(x_\gamma)} + 2m_e^2 x_\gamma \left(\frac{1}{Q^2_{\max}} - \frac{1}{Q^2_{\min}(x_\gamma)}\right)\right]$$

  where $Q^2_{\min}(x_\gamma) = m_e^2 x_\gamma^2 / (1 - x_\gamma)$

VFNS treatment of J/ψ+charm yield

CF, J.-P. Lansberg, H.-S. Shao, Y. Yedelkina, PLB 811 (2020) 135926

J/ψ+charm production follows from

- $\gamma + g \to J/\psi + c + \bar{c}$ @ $\alpha\alpha_s^3$ (3FS)
- $\gamma + \{c, \bar{c}\} \to J/\psi + \{c, \bar{c}\}$ @ $\alpha\alpha_s^2$ (4FS)

$$d\sigma_{\gamma c \to J/\psi + c} = \frac{1}{2\left(\hat{s} - m_c^2\right)} dx_c \, f_{c/p}(x_c, \mu_F^2) \times \overline{\left|\mathcal{M}_{\gamma c \to J/\psi c}\right|^2} d\Phi(p_\gamma, p_c \to P_{\mathcal{Q}}, p_c'),$$

with

$$f_{c/p}(x_c, \mu_F^2) = \tilde{f}_{c/p}^{(1)}(x_c, \mu_F^2) + \mathcal{O}(\alpha_s^2),$$

where

$$\tilde{f}_{c/p}^{(1)}(x_c, \mu_F^2) = \frac{\alpha_s}{2\pi} \log\left(\frac{\mu_F^2}{m_c^2}\right) \int_{x_c}^1 \frac{dz}{z} P_{qg}(z) f_{g/p}\left(\frac{x_c}{z}, \mu_F^2\right)$$

with AP splitting function $P_{qg}(z) = \frac{1}{2}\left[z^2 + (1-z)^2\right]$. Overlap CT to be subtracted from 3FS:

$$d\sigma_{\mathrm{CT},\gamma c \to J/\psi + c} = \frac{1}{2\left(\hat{s} - m_c^2\right)} dx_c \, \tilde{f}_{c/p}^{(1)}(x_c, \mu_F^2) \overline{\left|\mathcal{M}_{\gamma c \to J/\psi c}\right|^2} d\Phi(p_\gamma, p_c \to P_{\mathcal{Q}}, p_c').$$

$b \to J/\psi$ feed-down

CF, J.-P. Lansberg, H.-S. Shao, Y. Yedelkina, PLB 811 (2020) 135926

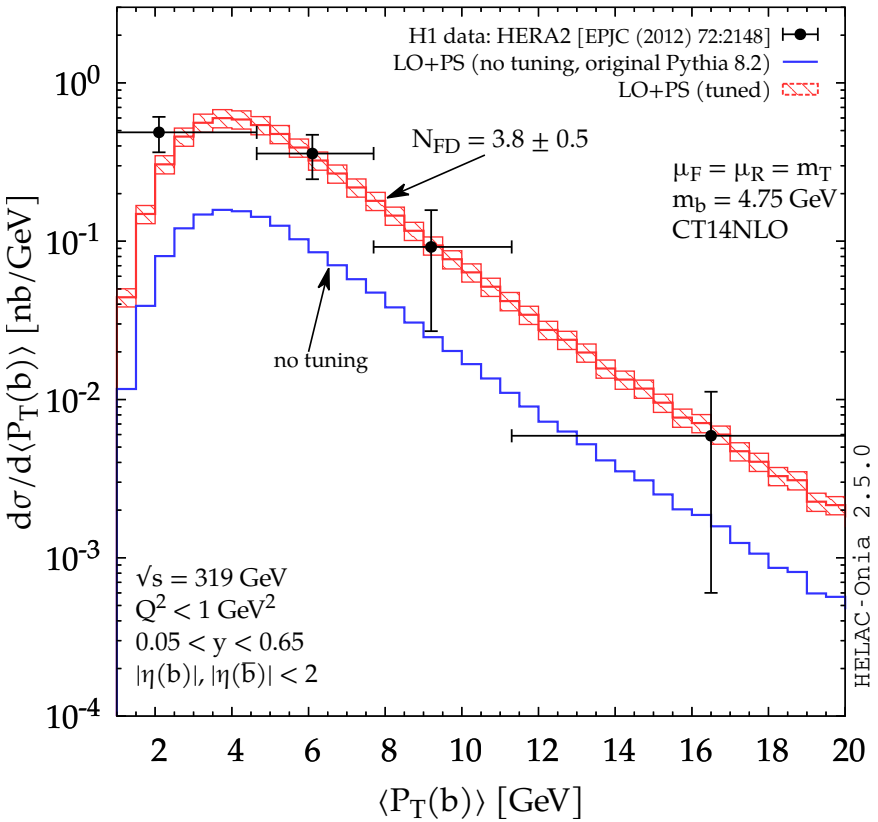

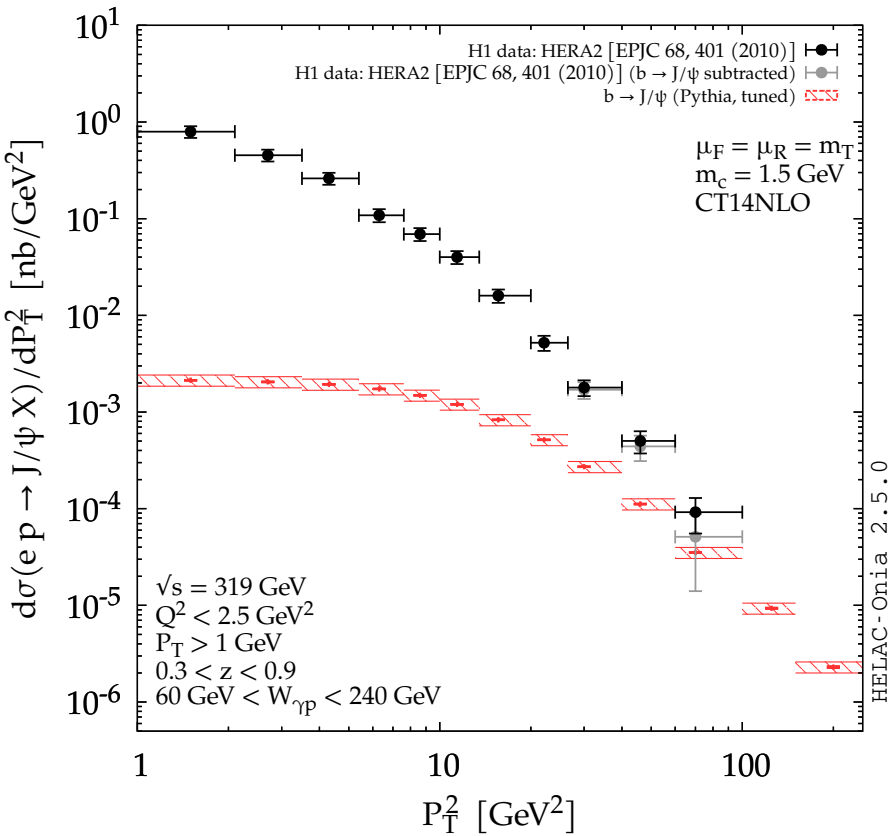

H1 $b\bar{b}$ production from **EPJC 72 (2012) 2148** [Note: $\langle P_T(b)\rangle = \sqrt{(P_{T,b}^2 + P_{T,\bar{b}}^2)/2}$]

$N_{FD} = 3.8 \pm 0.5$ estimated via χ^2-minimisation

$b \to J/\psi$ tuned with PYTHIA 8.2